



Since January 2020 Elsevier has created a COVID-19 resource centre with free information in English and Mandarin on the novel coronavirus COVID-19. The COVID-19 resource centre is hosted on Elsevier Connect, the company's public news and information website.

Elsevier hereby grants permission to make all its COVID-19-related research that is available on the COVID-19 resource centre - including this research content - immediately available in PubMed Central and other publicly funded repositories, such as the WHO COVID database with rights for unrestricted research re-use and analyses in any form or by any means with acknowledgement of the original source. These permissions are granted for free by Elsevier for as long as the COVID-19 resource centre remains active.



## Effects of COVID-19 era on a subtropical river basin in Bangladesh: Heavy metal(loid)s distribution, sources and probable human health risks



Jawad-Ul-Haque<sup>a</sup>, Md. Abu Bakar Siddique<sup>b</sup>, Md. Saiful Islam<sup>c</sup>, Mir Mohammad Ali<sup>d</sup>, Cem Tokatli<sup>e</sup>, Aznarul Islam<sup>f</sup>, Subodh Chandra Pal<sup>g</sup>, Abubakar M. Idris<sup>h,i</sup>, Guilherme Malafaia<sup>j,k,l</sup>, Abu Reza Md Towfiqul Islam<sup>a,\*</sup>

<sup>a</sup> Department of Disaster Management, Begum Bekeya University, Rangpur 5400, Bangladesh

<sup>b</sup> Institute of National Analytical Research and Service (INARS), Bangladesh Council of Scientific and Industrial Research (BCSIR), Dhanmondi, Dhaka 1205, Bangladesh

<sup>c</sup> Department of Soil Science, Patuakhali Science and Technology University, Dumki, Patuakhali 8602, Bangladesh

<sup>d</sup> Department of Aquaculture, Sher-e-Bangla Agricultural University, Dhaka 1207, Bangladesh

<sup>e</sup> Trakya University, Laboratory Technology Department, Ipsala, Edirne, Turkey

<sup>f</sup> Department of Geography, Aliah University, 17 Gorachand Road, Kolkata 700 014, West Bengal, India

<sup>g</sup> Department of Geography, The University of Burdwan, Bardhaman 713104, West Bengal, India

<sup>h</sup> Department of Chemistry, College of Science, King Khalid University, Abha 62529, Saudi Arabia

<sup>i</sup> Research Center for Advanced Materials Science (RCAMS), King Khalid University, Abha 62529, Saudi Arabia

<sup>j</sup> Post-Graduation Program in Conservation of Cerrado Natural Resources, Goiano Federal Institute, Urutaí, GO, Brazil

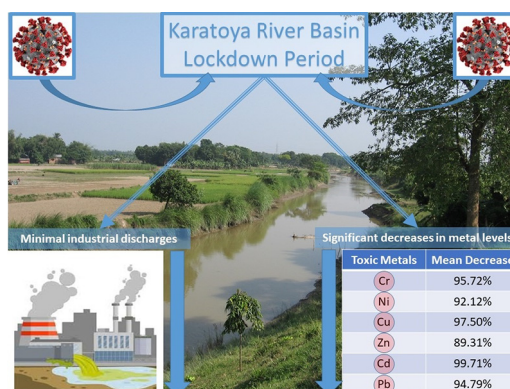
<sup>k</sup> Post-Graduation Program in Ecology, Conservation, and Biodiversity, Federal University of Uberlândia, Uberlândia, MG, Brazil

<sup>l</sup> Post-Graduation Program in Biotechnology and Biodiversity, Federal University of Goiás, Goiânia, GO, Brazil

### HIGHLIGHTS

- Identified significant reductions in elemental content during the post-lockdown
- Surface water pollution levels, assessed by pollution indices, were reduced by around 24 %.
- Irrigation indices revealed an improvement in the river water quality of up to 62 %.
- Children's and adults' carcinogenic risks were reduced serially by 54 & 53 % after lockdown.
- Domestic sewage increases pollution despite no industrial or agricultural effluents.

### GRAPHICAL ABSTRACT



### ARTICLE INFO

Editor: Damià Barceló

#### Keywords:

COVID-19 lockdown  
Surface water quality  
Irrigation water quality  
Carcinogenic risk  
Eco-restoration strategies

### ABSTRACT

The COVID-19 era has profoundly affected everyday human life, the environment, and freshwater ecosystems worldwide. Despite the numerous influences, a strict COVID-19 lockdown might improve the surface water quality and thus provide an unprecedented opportunity to restore the degraded freshwater resource. Therefore, we intend to investigate the spatiotemporal water quality, sources, and preliminary health risks of heavy metal(loid)s in the Karatoya River basin (KRB), a tropical urban river in Bangladesh. Seventy water samples were collected from 35 stations in KRB in 2019 and 2022 during the dry season. The results showed that the concentrations of Ni, Cu, Zn, Pb, Cd, and Cr were significantly reduced by 89.3–99.7 % during the post-lockdown period ( $p < 0.05$ ). However, pH, Fe, Mn, and As concentrations increased due to the rise of urban waste and the usage of disinfectants during the post-

\* Corresponding author at: Begum Rokeya University, Department of Disaster Management, Rangpur, Bangladesh.  
E-mail address: [towfiq\\_dm@brur.ac.bd](mailto:towfiq_dm@brur.ac.bd) (A.R.M.T. Islam).

lockdown phase. In the post-lockdown phase, the heavy metal pollution index, heavy metal evaluation index, and Nemerow's pollution index values lessened by 8.58 %, 42.86 %, and 22.86 %, respectively. Besides, the irrigation water quality indices also improved by 59 %–62 %. The total hazard index values increased by 24 % (children) and 22 % (adults) due to the rise in Mn and As concentrations during the lockdown. In comparison, total carcinogenic risk values were reduced by 54 % (children) and 53 % (adults) in the post-lockdown. We found no significant changes in river flow, rainfall, or land cover near the river from the pre to post-lockdown phase. The results of semivariogram models have demonstrated that most attributes have weak spatial dependence, indicating restricted industrial and agricultural effluents during the lockdown, significantly improving river water quality. Our study confirms that the lockdown provides a unique opportunity for the remarkable improvement of degraded freshwater resources. Long-term management policies and regular monitoring should reduce river pollution and clean surface water.

## 1. Introduction

The present pandemic era triggered by COVID-19 (coronavirus disease 2019) affected the entire globe within a short time and created the most significant challenge humanity has faced since World War II. This pandemic has unprecedentedly impacted daily human lives and reminded us how weak humans are (Bodrud-Doza et al., 2020). Considering the overall impact, the World Health Organization (WHO) proclaimed COVID-19 a “Public Health Emergency of International Concern” on January 30, 2020, and a pandemic on March 11, 2020. In the wake of these declarations, various restrictions are imposed on the normal daily lives of people, including solo travel, social distancing, isolation, lockdown, and so on, in most of the countries in the world to control the extensive spread of the coronavirus (Tokatlı and Varol, 2021). In Bangladesh, the first COVID-19-affected person was detected on March 8, 2020 (Shammi et al., 2020), and the first death occurred on March 18, 2020. To keep this syndrome from spreading and to protect the population, the Bangladesh government announced a “lockdown” in the whole nation from March 23 (effective March 26) to May 30, 2020, for the first time. The restrictions were gradually increased after the first period of lockdown.

Interestingly, these restrictions have some positive impacts on nature, along with control of the spread of disease. The overall natural environmental conditions in the world, including Bangladesh, have improved significantly as a result of controlled traffic and industrial operations (Ali et al., 2020; Bao and Zhang, 2020; Sharma et al., 2020; Collivignarelli et al., 2020; Otmani et al., 2020; Aydın et al., 2020; Dantas et al., 2020; Chakraborty et al., 2021). In normal conditions, industries discharge many untreated or improperly treated effluents into the adjacent environment, mainly into the river systems (Ahsan et al., 2019; Kubra et al., 2022). However, the lockdown has been attributed to the reduction of the release of industrial effluents into the surface water bodies, which ultimately improved the surface water quality after the COVID-19 lockdown period (Yunus et al., 2020; Arif et al., 2020; Dutta et al., 2020; Aman et al., 2020a; Karunanidhi et al., 2022; Khan et al., 2021a; Rendana et al., 2022). For instance, the Yamuna and Ganga rivers' (India) water exhibited significant improvements in biochemical and chemical oxygen demand and dissolved oxygen attributes in the post-lockdown period (Dutta et al., 2020; Patel et al., 2020; Shukla et al., 2021). Moreover, Yunus et al. (2020) found higher surface water transparency in the Venice Lagoon. The countrywide lockdown executed to curb the expanse of COVID-19 in Bangladesh may have probably led to enhancing the water quality of a tropical urban river. Due to the imposed restrictions on industrial and other human influences in the river basin, the amount of industrial effluent discharged into the river water has been reduced. Thus, heavy metal contamination levels in the river water might be reduced. However, an in-depth investigation is needed to evaluate whether the above statement is correct and what the actual condition is. Therefore, we sampled the Karatoya River water in the Bogura District of Bangladesh in mid-February 2020 (pre-lockdown period) and early January 2022 (post-lockdown period). We measured the levels of heavy metal concentrations. This opens the door for us to a chance to compare the water quality of the tropical river basin before and after the COVID-19 lockdown periods.

In developing countries like Bangladesh, with limited freshwater resources, the rivers contribute to the environment significantly and play multiple roles in the ecological systems and human life (Jin et al., 2019). Surface water is the most critical inland resource for human consumption, agricultural operations, and recreational and industrial uses (Islam et al., 2022). On the globe, surface water is an essential component of life; unfortunately, it is the most threatened resource due to the over-extraction of rising populations, intensive activities from agriculture, unplanned urbanization, the transformation of land cover, and climate change (Kim et al., 2018; Kumar et al., 2022). In recent decades, safe drinking water has been one of the essential requirements to meet the United Nation's Sustainable Development Goals (SDGs) for ensuring good public health, livelihoods, and food security (Sojobi, 2016). SDG-6 aims to provide all Bangladeshis with sustainable fresh water and sanitation management by 2030 (UN Water, 2018). Presently, >80 % of the total population in Bangladesh lacks clean and safe drinking water resources (Yeazdani, 2016) due to the existence of trace elements like Cr, Cd, Pb, As, Cu, and Ni, etc., which are making it harder to achieve the SDS-6 goal (UNICEF, 2009). In Bangladesh, a considerable amount of waste from various sources, including household, medical, and industrial waste, is discharged regularly into the surface water systems (Islam et al., 2020; Siddique et al., 2022). The Karatoya River, connected to the Teesta and Brahmaputra Rivers, runs through the Bogura district in northern Bangladesh. Recently, extreme pollution in the Karatoya River has raised concern among the public (Islam et al., 2015; Proshad et al., 2022; Khan et al., 2022). Rapid industrial growth and unplanned urbanization are deteriorating the quality of surface water by releasing a massive amount of pollutants such as toxic elements (As, Cd, Cr, Cu, Fe, Hg, Mn, Ni, Pb, and Zn) into the nearby river basin from various sources, thus posing a severe threat to the river ecology as well as human health (Kazakisa et al., 2020; Ge et al., 2021; Xiong et al., 2021). Most living creatures face momentous health consequences due to non-biodegradable toxic metals (Chen et al., 2021; Dash et al., 2021; Li et al., 2021). In recent decades, due to the exponential growth of the world economy and population, a spate of environmental challenges has resulted (Sun et al., 2019; Nguyen et al., 2020; Ustaoglu and Islam, 2020). In this regard, the contamination of aquatic ecosystems (i.e., reservoirs, lakes, tributaries, rivers) by toxic elements is particularly noticeable since metals are persistent pollutants that can never be destroyed and impose significant risks on ecology and human health (Liu et al., 2019; Sun et al., 2019; Nguyen et al., 2020).

According to previous literature, a substantial number of studies have already been conducted around the world demonstrating the impacts of COVID-19 lockdown on river water quality (Chaurasia et al., 2020; Shah et al., 2020; Mukherjee et al., 2020; Aman et al., 2020b; Pant et al., 2021; Custodio et al., 2021; Chakraborty et al., 2022; Hagnazar et al., 2022; Tokatlı et al., 2022). For example, Tokatlı and Varol (2021) investigated the influence of the lockdown in the Meric-Ergene River Basin of Northwest Turkey. Duttagupta et al. (2021) also investigated the effect of lockdown, due to the COVID-19 pandemic, on the Ganges River Basin, India. These studies used heavy metal pollution indices to show the pollution level and evaluated the associated health risks in those regions. However, they did not appraise the quality of river water for irrigation purposes, considering the lockdown impact of COVID-19 on agricultural sectors where surface

water, mainly from the rivers, is utilized for crop production and other associated agrarian activities. Similar studies have also been carried out by Sarkar et al. (2021a) and Haghazadeh et al. (2022) to find out the lockdown influence of COVID-19 on river water. In addition to the study of lockdown's effect on water quality, they assess the river's quality for use for irrigation purposes in both pre-and post-lockdown phases. However, the authors did not study the COVID-19 lockdown's impact on river water quality through proper systematic investigation. In Bangladesh, a study was conducted by Nasher and Islam et al. (2021) to grasp the effects of the COVID-19 lockdown on the turbidity of water in a highly polluted lake in the capital city of Dhaka. However, their study was limited based on the measured water quality parameters.

Furthermore, Bangladeshi people have already been exposed to heavy metals that cause significant health concerns due to contaminated drinking water (Singh et al., 2008; Uddin and Huda, 2011; Islam et al., 2022). When heavy metals enter the water system, they not only reduce the quality of water but also threaten the health of people and other organisms through ingestion and dermal exposure pathways (Habib et al., 2020; Siddique et al., 2022; Nasher and Islam, 2021). The paths of these exposures are linked to various heavy metal-impacted diseases, e.g., kidney damage, malformation, cancer, and even death due to the elevated toxic element concentrations in the water (Hasanuzzaman et al., 2017a; Islam et al., 2022). The pioneering attempt in Bangladesh's heavily polluted urban river context will contribute to a global holistic understanding of the integrated nature of human-environment interactions. Higher control should be exerted on restricting the accelerated rate of anthropogenic interventions on aquatic ecosystems through promoting pro-environmental behavior at the individual and societal level rather than damaging the ecosystem and its subsequent restoration with massive monetary involvement. This approach embraced in this study will undoubtedly enhance the scientific knowledge worldwide concerning sustainable eco-restoration practices in water resources management and attain sustainable development goals, primarily SDG 6 related to clean water and SDG 14 on life underwater. So, it is vital to know the status of river water quality in the first instance and then adopt the appropriate measures to prevent further surface water contamination through proper assessment of river water quality and continuous monitoring. From the previous study on heavy metal(loid)s in surface water, it was clear that the effects of the COVID-19 lockdown were not examined to measure the quality of the surface water in Bangladesh.

In Bangladesh, systematic studies on the impacts of lockdown due to COVID-19 on heavy metal(loid)s contamination and its adverse health consequences, irrigational water quality status, trace element concentration and their co-distribution, and the origins of heavy metals (loids) in surface water in urban rivers are very scarce. Therefore, considering the significant impact of the COVID-19 lockdown in Bangladesh, our study intends to design an integrated approach to (i) assess heavy metal(loid)s contamination in the surface water of an urban river in Bangladesh during pre- and post-lockdown phases through heavy metal pollution indices; (ii) evaluate the quality of the water for irrigational uses; (iii) quantify the origin of heavy metal(loid)s in the river water with multivariate statistics in compositional data analysis (CDA) framework; (iv) assess the human health risks due to water's heavy metal(loid)s contamination; and (v) study the temporal and spatial distributions of heavy metal(loid)s in the study basin using geostatistical modeling and GIS (Geographic information systems) tools. To assess the surface water contamination by heavy metal(loid)s due to the COVID-19 lockdown, the heavy metal pollution index (HPI), heavy metal evaluation index (HEI), and Nemerow's Pollution Index (NPI) are implemented for the proper assessment. Irrigation water quality assessment is employed to determine the impacts on water quality for irrigation use during the pre-and post-lockdown periods through evaluating sodium adsorption ratio, magnesium rate, and Kelly's index. To quantify the possible sources and factors controlling the river water quality in both phases, multivariate statistics such as CDA, cluster analysis (CA), and Pearson's correlation index (PCI) were used for this purpose. Assessment of human health risks was performed by the evaluation of Hazard Quotients (HQs), Hazard Index (HI), and Cancer Risk (CR) of the tested water-quality attributes for

both age groups (adults and children). The traditional health risk model employed by the U.S. Environmental Protection Agency (USEPA) is generally used to evaluate the possible risks to human health. To the best of the authors' knowledge, this is the first assessment of the COVID-19 lockdown's impacts on the surface water quality of an urban tropical river in Bangladesh. We have scientifically demonstrated the contamination of heavy metal(loid)s in the river water with multiple heavy metal pollution indices, appraised the associated health risks of heavy metal(loid)s, and appraised the irrigational water quality and factors influencing the water contamination with their sources. The outcomes of our study will provide important information about how the COVID-19 lockdown affected the quality of surface water and public health. This information can also be used as a model for the other urban areas of Bangladesh.

## 2. Materials and methods

### 2.1. Study area

The Karatoya River originates in the Himalayas and flows over the northern parts of Bangladesh. The Karatoya River is found in Bangladesh's Rajshahi division, in the southern portion of the country (Fig. 1). For this study, the part of the Karatoya river that flows through the urbanized area of the Bogura district was selected. The total zone of the Bogura district is about 2899 km<sup>2</sup>. According to the 2011 Bangladesh census, the population of this district is approximately 3,400,874 (Bangladesh Bureau of Statistics (BBS), 2020). The designated area is positioned in the northern region of Bangladesh (Fig. 1). The annual rainfall of the study area fluctuates seasonally, with substantial peaks occurring from June to August and dry spells occurring from October to February. As per the given information from the Department of Environment of Bogura district, the average annual rainfall is 1450 mm. The relative humidity in the study basin ranges from 61 % in March to 80 % in October. The wet season in Bogura is hot, humid, and gloomy, whereas the dry season is mild and usually clear. The average high temperature is 31.8 °C, and the average low temperature is 10.5 °C (Islam et al., 2015).

Along its 200-km path, hundreds of villages, towns, and commercial places have been built on both sides of the Karatoya River. Bogura is one of the fastest-growing industrialized cities with various small and medium-sized industries (Islam et al., 2015). The capital of ancient Pundranagar, Mohasthangarh, still stands beside the Karatoya River as a symbol of ancient history in Bangladesh. The river is related to agro-farming practices, fishing, and sea transportation that contribute substantially to the nation's economy (Proshad et al., 2022). The Karatoya River is very polluted because it takes in pollution from many sources and gets trash and waste from many places during the dry season. Because the air is dry and humid and the days are hot, hazardous leachate from the landfill flows into the river. Due to rain and surface runoff in agricultural fields, farm waste ends up in the Karatoya River, making it more polluted. In brickfields, ready-made garments, food, dyeing, metal, agrochemical industries, poultry feeding, and leather tanning industries have been built in recent decades (Zakir et al., 2013). This river receives household waste, domestic raw sewage, and industrial waste from the surrounding area (Islam et al., 2020). Human activities have resulted in a significant decline in river ecosystems over the last few decades. Every year, thousands of tons of untreated industrial and household waste are dumped in the river basin, which creates a critical concern for the typical river ecosystem and associated human and agricultural activities (Islam et al., 2015). These wastes could contain a large volume of toxic metals and pose an ecological risk to the riverine environment.

The study area is characterized by two typical landforms: (a) the Barind tract, and (b) the floodplains. The pre-Holocene sediments cover by the Barind Tract and the Holocene unconsolidated sediments encompass the remaining floodplain area (Reimann, 1993). Hydrogeologically, the study area consists of semi-impervious recent Pleistocene clayey silt aquitard (thickness varied from 3.0 to 47.5 m) which overlays a single- to multiple-layered (ranged from 2 to 4 m) aquifer system of Plio-



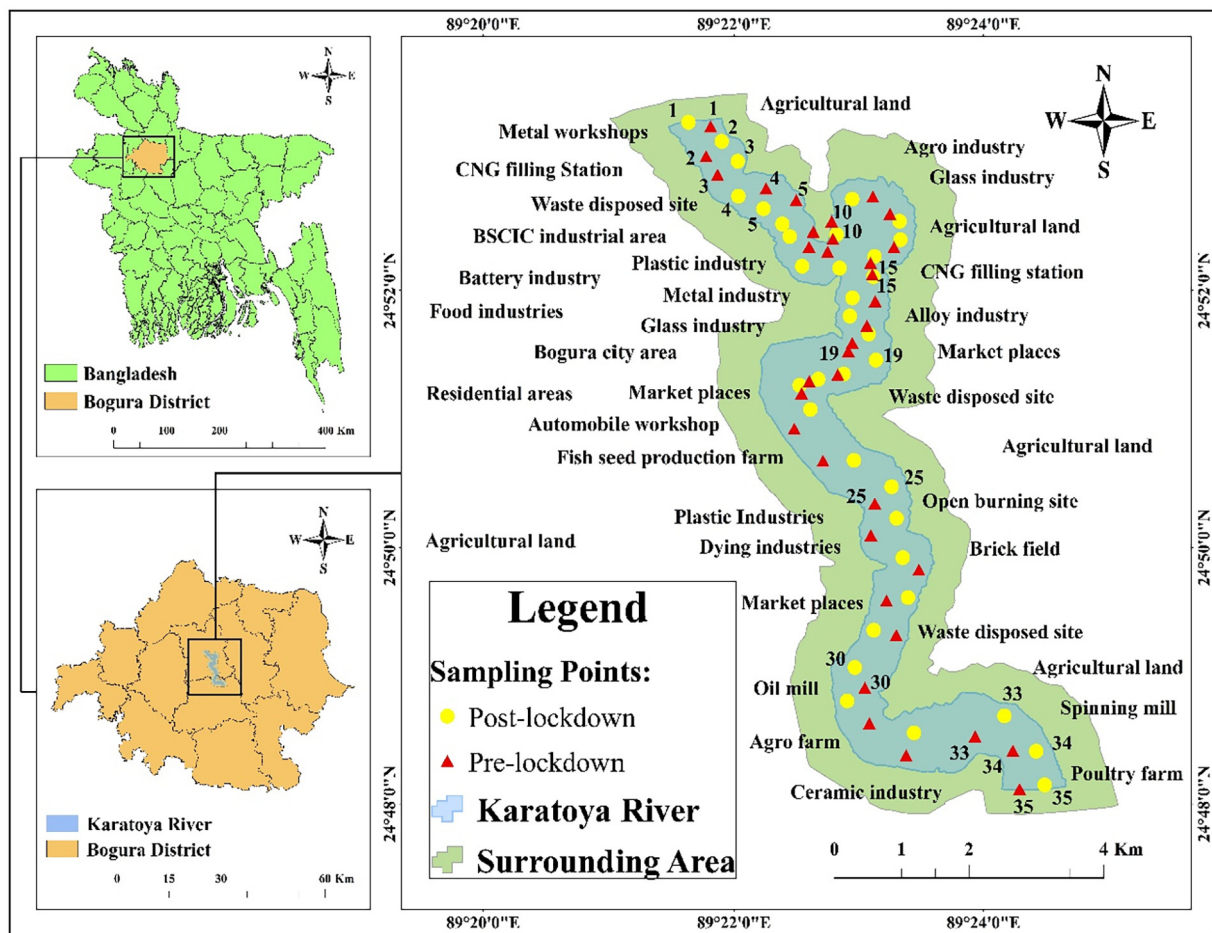


Fig. 1. Study area showing sampling locations in the Karatoya River basin, Bogura district, Bangladesh.

Pleistocene age (Hasanuzzaman et al., 2017b). The Holocene aquifers are normally unconfined or semi-confined nature but the pre-Holocene aquifers are mainly confined to semi-confined (DPHE (Department of Public Health Engineering), 2001). The permeability of Holocene aquifer is greater than that of pre-Holocene aquifer. The lithology is highly variable both in horizontal and vertical portions generating localized and highly heterogeneous aquifers (DPHE (Department of Public Health Engineering), 2001). Besides, the subsurface lithology contains mainly clay to silty clay at the upper-most layer and fine to coarse sands at lower-most layer. Geologically, the study area is dominated by the Bogra shelf under the Precambrian Rangpur platform of Bengal basin, Bangladesh (Jahan et al., 2005). The texture of the soil is predominantly silty loam and clay loam in the study basin.

## 2.2. Sampling and analysis

A total of 35 composite samples of river water were collected from the Karatoya River basin in Bogura district, Bangladesh, in both the pre-lockdown (mid-February 2020) and post-lockdown (early January 2022) phases. For each period, the samples were collected from the upstream to the downstream of the flowing Karatoya River (Fig. 1). The unfiltered samples from the river water were primarily taken from the center part of the Karatoya River, at a depth of about 20 cm beneath the surface of the river water. From each sampling point, 2–3 replicate water samples were taken into 500 mL acid-washed non-transparent polyethylene plastic bottles and mixed well to obtain the composite sample. The sampling water of the respective points was used to wash the bottles thoroughly before taking the samples to avoid any possible unwanted preexisting contamination from the bottles. After collecting the water samples in the bottles, 1 mL of

ultrapure nitric acid (68 %) was immediately used to resist the precipitation or loss of metals chemically and biologically. In the field, pH, dissolved oxygen (DO), and total dissolved solids (TDS) were determined with a portable multimeter (Lutron-2015). The pH meter used in the measurement was calibrated with pH 4 and pH 7 standards. The concentrations of the 12 chemical elements (Na, Mg, Ca, Cu, Fe, Mn, Zn, Pb, Ni, Cd, Cr, and As) were estimated in the laboratory by inductively coupled plasma-mass spectrometry (ICP-MS, Agilent 7700). For this purpose, a small portion of the collected composite river water samples was filtered and filled into the small plastic sample vials. The samples in the vials were then directly used in the analysis by the ICP-MS instrument. For higher concentrations of chemical parameters in the samples, the river water samples were diluted, whereas, for lower contents, the samples were concentrated to analyze the parameters within the operating range of the calibration curve.

## 2.3. Data validation and quality assurance

During the analysis of chemical elements using the ICP-MS, the quality of the obtained data was ensured in several ways, such as by determining the samples in duplicates, analyzing the spiked samples and checking standards, and measuring the method blanks. All chemicals were of analytical grade, and high-quality deionized water (conductivity  $<0.2 \mu\text{S}/\text{cm}$ ) was utilized to prepare samples and standards. For the proper outcome, highly pure (purity: 99.98 %) NIST (National Institute of Standard and Technology) traceable ISO-certified reference material (Fluka Analytical, Sigma-Aldrich, Germany) was used for constructing the calibration curves of the target elements, and the concentration of the elements was determined against the obtained linear calibration curves ( $R^2 > 0.999$ ). The relative standard deviation (RSD) for each duplicate determination of the analyzed

samples was <5 %. The spike recovery in the elements analysis was 95.7–101.0 % for the samples of the pre-lockdown period and 99.2–100.4 % for the post-lockdown period (Table S1). The ICP-MS instrument was instructed to analyze each sample in a triplicate fashion, and the triplicate measurement's mean value (RSD < 5 %) was reported. During the analysis period, the precision of the analysis was rechecked by the measures of the certified reference material in triplicates as unknown samples. Measurement comparison of the samples was made with the elements' certified values (Table S1). In every case, the analyzed data was close to the certified values. This made the analysis even more accurate and precise.

2.4. Metal pollution indices

Three indices were used to evaluate water quality by its heavy metal (loid)s content in the Karatoya River (Bangladesh). The HPI, HEI, and NPI were used in our study, considering their wide use and acceptability in recent studies (e.g., Zhao et al., 2022; Karunanidhi et al., 2022; Mukherjee et al., 2020). The HPI, HEI, and NPI methods were introduced to assess the overall quality of water by adding heavy metal(loid)s. The HPI index considers the relative toxicity of each metal by assigning a weighting factor or a rating to each selected attribute. In the calculation of HPI in our study, the concentration limits, that is, the allowed guideline value and the most desirable value for each parameter, were extracted from the WHO standards. On the other hand, the HEI was used to synchronize the criteria for different pollution indices. The NPI was used to determine the overall pollution level. Because various heavy metal(loid)s may have other effects on the same site, this technique may offer a valid assessment of heavy metal (loid)s contamination at each location (Yan et al., 2016). The details of the pollution indices (HPI, HEI, and NPI) are provided in Table 1.

2.5. Irrigation water quality assessment

The sodium absorption ratio (SAR), magnesium rate (MR), and Kelly's index (KI) were utilized to measure the irrigational water quality in the study region. The SAR is an essential indicator for measuring the concentration and potential for sodium risks in Ca<sup>2+</sup> and Mg<sup>2+</sup> (Shammi et al., 2022). The MR index was developed by Paliwal (1972) for calculating the magnesium hazard in irrigated water. Kelly's index (KI) compares the content of sodium in soil and water to the content of Mg<sup>2+</sup> (Kelly, 1940). Table 1 displays the SAR, MR, and KI irrigation water quality indices.

2.6. Human health risk evaluation

Risk evaluation is a combination of hazard and exposure. It is described as determining the likelihood of any given quantity of unfavorable health consequences occurring over a particular period (Bortey-Sam et al., 2015). Each metal (loid) health risk evaluation is often based on a measurement of the risk level, represented in terms of carcinogenic and noncarcinogenic health risks (USEPA (US Environmental Protection Agency), 2009). The health risks is assessed for the two age groups, including children and adults. According to the water consumption pathways, the noncarcinogenic risk is calculated for both the oral and dermal ways. The Hazard Quotient (HQ), Hazard Index (HI), and Carcinogenic Risk (CR) are used for evaluating the health risks of heavy metal(loid)s contamination in the surface water of the study area. The specifics of the human health risk assessment (HQ, HI, CR) are given in Table S2. Heavy metal(loid) exposure parameters of heavy metal(loid)s through oral ingestion and dermal pathways are represented in Tables S3, S4, and S5.

2.7. Geostatistical modeling and spatial interpolation

Geostatistical modeling is widely practiced in the spatial interpolation of an attribute. In the present context, we applied semivariogram models for assessing the best-fit models for depicting the spatial distribution of the chemical species and various indices used in the current analysis. Following Journel and Huijbregts (1978), the semivariogram may be computed using Eq.1

$$\gamma(h) = \frac{1}{2n} \sum_{i=1}^n [\zeta(x_i) - \zeta(x_i + h)]^2 \tag{1}$$

where n stands for pair numbers of sample points divided by the standard distance called lag h, z(xi) denotes the value of variable z at the location of xi.

Several semivariogram models could potentially show a distribution with a minimum error (Hu et al., 2004). However, the choice of the best fit models is based on the minimum mean error (ME), mean standard error (MSE), root mean square error (RMSE), average standard error (ASR), and root mean square standardized error (RMSSE). The computation of these error factors was performed using the 'geostatistics' module of the ArcGIS software (v. 10.2). Thus, the search for best-fit models entails selecting the main interpolation techniques and their best-fit statistical distribution. For the present study, ordinary kriging (OK), simple kriging (SK),

**Table 1**  
Mathematical expressions and contamination degree of heavy metal pollution and irrigation water quality indices.

Index	Calculation	Formula explanations	Contamination degree	References
Heavy metal pollution index (HPI)	$Q_i = \sum_{i=1}^n \frac{M_i}{S_i} \times 100$ $HPI = \frac{\sum_{i=1}^n W_i Q_i}{\sum_{i=1}^n W_i}$	Q <sub>i</sub> : The sub-index of the toxicant W <sub>i</sub> : The unit weight of the i <sub>th</sub> parameter M <sub>i</sub> : The monitored values of toxicant S <sub>i</sub> : The standard values	HPI < 100: Low heavy metal pollution HPI > 100: High heavy metal pollution	Mohan et al., 1996
Heavy metal evaluation index (HEI)	$HEI = \sum_{i=1}^n \frac{H_c}{H_{MAC}}$	H <sub>c</sub> : The value observed for each parameter H <sub>MAC</sub> : The limit value for each parameter	HEI < 10: Low pollution 10–20: Medium pollution HEI > 20: High pollution	Edet and Offiong, 2002
Nemerow's pollution index (NPI)	$NPI = \sqrt{\frac{(\max Pi)^2 + (\bar{Pi})^2}{2}}$	max Pi: is the maximum single pollution index Pi: is the mean of single pollution indexes	NPI ≤ 1: clarity of the water 1 < NPI ≤ 2.5: low clarity 2.5 < NPI ≤ 7: moderate pollution NPI > 7: high pollution	Yan et al., 2016
Sodium absorption ratio (SAR)	$SAR = \frac{Na}{\sqrt{\frac{Ca+Mg}{2}}}$	Na: concentration of Sodium Ca: Concentration of Calcium Mg: Concentration on Magnesium	SAR < 20 Excellent 20–40 Good 40–60 Permissible 60–80 Doubtful SAR > 80 Not applicable	Richards, 1954
Magnesium rate (MR)	$MR = \left( \frac{Mg}{Mg+Ca} \right) \times 100$	Mg: Concentration on Magnesium Ca: Concentration of Calcium	MR < 50: Suitable MR > 50: Not suitable	Paliwal, 1972
Kelly's index (KI)	$KI = \frac{Na}{Mg+Ca}$	Na: concentration of Sodium Ca: Concentration of Calcium Mg: Concentration on Magnesium	KI < 1: Suitable KI > 1: Not suitable	Kelly, 1940

and inverse distance weight (IDW) with various semivariogram models such as spherical, power 1, power 2, exponential, Gaussian, and circular were found to be suitable models for the different distributions. The computation of the OK, SK, and IDW is expressed using Eq. 2–4 following Ghanbarpour et al. (2013), (Goovaerts, 1997), and (Goovaerts, 2000).

$$\hat{z}(x_0) = \sum_{i=1}^n \lambda_i z(x_i) \tag{2}$$

$$\hat{z}(x_0) = m + \sum_{i=1}^n \lambda_i [z(x_i) - m] \tag{3}$$

$$\lambda_i = d_{i0}^{-p} \sum_{i=1}^n d_{i0}^{-p} \tag{4}$$

where  $\hat{z}$  stands for the measured value at the sampled point  $x_0$ ,  $z$  denotes the observed value at point  $x_i$ ,  $\lambda_i$  depicts the weight assigned to the point, and  $n$  shows the sampled number used for the estimation,  $m$  stands for mean,  $d_{i0}$  represents the distance between the sample locations and the prediction points and  $p$  for power parameter.

### 2.8. Statistical analysis

Several descriptive statistical approaches were used to analyze statistical variables such as maximum, minimum, mean, and standard deviation for the surface water quality dataset. The concentration of a given element expresses a part of a whole in the compositional nature of hydrochemical data. In geochemistry and statistics, these concentrations are known as “closed data,” which implies that they do not vary independently. Consequently, they are not well represented by the usual Euclidean mathematical structure. This may lead to essential drawbacks in the principal component analysis (PCA) analysis, including the cross-correlations, which different authors have widely discussed (Buccianti and Grunsky, 2014; Filzmoser et al., 2018; Pawlowsky-Glahn et al., 2015; Herms et al., 2021, among others). We conducted the PCA analysis in a compositional data (CODA) framework in such a case. We applied HJ-Biplot to display the data collected in the current research, which has some benefits; for instance, it simultaneously enables the examination of multiple variables in the same graphical representational plane. Besides, it allows for individual and group comparisons. Because compositional data contains positive natural components, retraining the data attributes and inter-element relationships is required before using multivariate analysis on geochemical datasets. Log-ratio transformations have been reported in the literature to treat data structures by deploying multivariate statistics (Reimann et al., 2012). Over the last few decades, many researchers have used factor analysis (FA), an excellent way to find pollution from hypothetical sources (Herms et al., 2021; Kumar et al., 2021).

Basic statistical analysis, such as the testing for normality and equal variance of data, was performed using SPSS 22.0 (IBM Corp., Armonk, NY, USA). The data were first examined for normality using the Kolmogorov-Smirnov (KS) test. The identification of potential factors that affect river water quality in the study area was carried out by PCA/FA in both phases. The PCA/FA, Bartlett’s sphericity test, and Kaiser-Meyer-Olkin (KMO) test were employed to examine the suitability of the datasets before starting the analysis (Ustaoğlu and Tepe, 2019).

## 3. Results and discussion

### 3.1. Physicochemical attributes and heavy metal(loid)s

The general characteristics of the surface water samples from Karatoya River, Bogura district, during pre-lockdown and post-lockdown were statistically analyzed. General attributes such as pH, TDS, DO, Na, Mg, Ca, and heavy metal(loid)s including Fe, Mn, Zn, Cu, Cr, Cd, Pb, and As were present in the samples. Statistical clarification of these attributes is given in Table 2. Table 2 also revealed the comparison of the minimum, maximum, and mean concentrations of these attributes in both periods (pre- and post-lockdown) with the drinking water guideline values by Bangladesh Water Quality Standards (DoE (Department of Environment and Government of the People’s Republic of Bangladesh), 1997) and the World Health Organization (WHO, 2011). The results indicate that most surface water quality attributes do not exceed the standards (BDWS & WHO) except for some attributes. The differences (%) between pre-and post-lockdown are shown in Fig. 2. The differences between these times show that most of the high concentrations decreased after the lockdown, except for Fe, Mn, and As, whose average levels increased slightly due to the use of agro-chemicals, particularly arsenic sulfide, while tanning leather and treating wood with copper arsenate (Islam, 2021). The elevated As is found in river water, mostly from upland Himalayan foothills that are linked to the Koratoya River in northern Bangladesh (Khan et al., 2021b). Chemical weathering and erosion of the Himalayan foothills have an impact on the distribution of metal(loid)s inflow into sediments transported by rivers and groundwater circulation (Khan et al., 2022). Due to the fine-grained sediments, Fe, Mn, and As concentrations rise on the downstream side of the Koratoya River. Arsenic levels are higher in the finer sediments on the downstream side of the study area as Fe and Mn levels rise as well.

Fig. 2 shows that the distributions of Mn are high in the northwestern and southwestern parts of the riverine area in the pre-lockdown phase. During the post-lockdown periods, the spatial distributions show the high Mn concentration decreasing but the number of contaminated zones increasing. This might have happened due to domestic waste dumping during

**Table 2**  
Descriptive statistics table of the physicochemical and chemical attributes evaluated in Karatoya River (Bangladesh).

Attributes	Measurement units	Pre-lockdown			Post-lockdown			Difference	Difference (%)	Standards	
		Minimum	Maximum	Mean	Minimum	Maximum	Mean			BD (DoE (Department of Environment and Government of the People’s Republic of Bangladesh), 1997)	WHO (2011)
Temperature	°C	21.4	28.4	24.4	21.1	27.6	24.2	0.20	0.82		
pH	–	5.13	7.22	6.20	5.95	7.62	6.96	0.76	12.3	6.5–8.5	6.5–8.5
TDS	mg/L	12.5	151.1	80.35	15.1	128.7	69.59	–10.77	–13.4	1000	1000
DO	mg/L	4.68	13.5	8.12	5.51	11.44	7.97	–0.16	–1.9	6.5–8	
Na	µg/L	26,600	89,200	54,534.3	8565	37,970	14,887.7	–39,646.6	–72.7	200,000	200
Mg	µg/L	4590	10,600	7258.3	5125	12,390	6973.1	–285.1	–3.90	30,000–35,000	50,000
Ca	µg/L	26,900	63,100	45,770	17,300	47,100	26,808.6	–18,961.4	–41.4	75,000	
Fe	µg/L	36	1981	884.5	99	8462	1997.8	1113.3	125.9	300–1000	300
Mn	µg/L	11	351	118.9	13	1377	366.5	247.6	208.3	100	400
Ni	µg/L	54.2	411.2	146.7	3.14	18.87	11.56	–135.11	–92.1	100	
Cu	µg/L	25.7	563	154.5	1.34	16.12	3.87	–150.6	–97.5	1000	
Zn	µg/L	22.6	550.6	181.4	6.70	56.2	19.40	–162.0	–89.3	5000	
Pb	µg/L	20.5	122	67.78	0.43	14.13	3.53	–64.25	–94.8	10	10
Cd	µg/L	9.80	74.6	33.71	0.008	0.303	0.10	–33.62	–99.7	5	3
Cr	µg/L	45.8	887	161.3	5.27	10.19	6.91	–154.4	–95.7	50	
As	µg/L	11.0	98.6	55.23	14.88	99.63	58.07	2.85	5.20	50	10



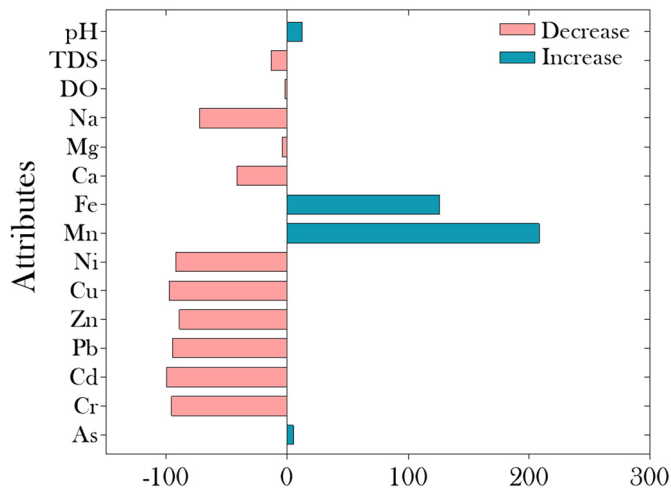


Fig. 2. Difference (%) among the water quality attributes during pre- and post-lockdown periods in Karatoya River (Bangladesh). TDS: total dissolved solids (mg/L); DO: dissolved oxygen (mg/L). The concentrations of chemical elements are expressed in  $\mu\text{g/L}$ .

the lockdown phase. The study area's northwest and middle parts show a high concentration of Mn in the post-lockdown periods.

The higher concentrations of Ni during pre-lockdown periods were noticed in the northeastern part of the basin. This area is surrounded by many different industries, including the metal industries (Islam et al., 2022). During the post-lockdown periods, all the highly contaminated zones in the northeastern part showed a low level of Ni concentration. This indicates that Ni mainly came into the river basin from anthropogenic sources. During the lockdown, when industrial activity is limited or stopped, the amount of Ni in those areas goes down.

On the other hand, Cu concentrations revealed that similar highly contaminated zones were found in the northwestern part of the basin during the pre- and post-lockdown periods. This might occur due to the waste dumping site beside the river basin and the industries operating during the lockdown periods (Haghnazar et al., 2022). However, the overall concentration of Cu was reduced in the post-lockdown periods. The higher content of Zn during the pre-lockdown period is noticeable in the northeastern part of the basin. Moreover, the southern part of the basin also had a higher concentration in the pre-lockdown period. But in the post-lockdown period, all the higher contaminated zones were reduced. Besides, the high water flow in the Koratoya River during the pre-lockdown period may cause physical disturbances that may accelerate the release of toxic metal(loid)s from the sediment to the water above, resulting in higher levels of Ni, Cu, Mn, and Zn in the surface water (Islam et al., 2015).

The mean temperature of the water samples was  $24.44\text{ }^{\circ}\text{C}$  in the pre-lockdown and  $24.27\text{ }^{\circ}\text{C}$  in the post-lockdown phases. The average TDS in the study area was  $80.4\text{ }\mu\text{S/cm}$  and  $69.6\text{ }\mu\text{S/cm}$  in the two phases, respectively. According to DoE (Department of Environment and Government of the People's Republic of Bangladesh) (1997) and WHO (2011) standards, the maximum permissible limit of TDS is  $1000\text{ }\mu\text{S/cm}$ . TDS primarily derives from agricultural and urban runoff, clay-rich streams, soil-polluted leaching, and industrial or sewage treatment plant point-source surface water pollution (Karunanidhi et al., 2022). The water temperature, ionic content, and types of ions in the surface water are mainly responsible for the variation of TDS in surface water (Chakraborty et al., 2021). The pH is below the acceptable limit of BDWS (1997) and WHO (1998) standards in the pre-lockdown phase but found within the acceptable limit in the post-lockdown phase. The average pH indicates that the surface water is slightly acidic in the pre-lockdown period and neutral after the COVID-19 lockdown. This change may occur due to the closing or limitation of industrial activity, less waste disposal from markets or bazaars, and various restrictions related to human activity in the river during the COVID-19

lockdown periods. The pH of water reflects its ability to react with acidic or alkaline substances in the water (Hem, 1991).

Furthermore, the concentrations of the heavy metal(loid)s are As (mean value of  $55.23\text{ }\mu\text{g/L}$ ), Zn (mean value of  $181.4\text{ }\mu\text{g/L}$ ), and Mn (mean value of  $118.9\text{ }\mu\text{g/L}$ ) in the pre-lockdown periods and As (mean value of  $58.07\text{ }\mu\text{g/L}$ ), Zn (mean value of  $19.4\text{ }\mu\text{g/L}$ ) and Mn (mean value of  $366.5\text{ }\mu\text{g/L}$ ) are observed in the post-lockdown periods. Among heavy metal(loid)s, Fe has a higher mean value in the post-lockdown period ( $1997.8\text{ }\mu\text{g/L}$ ) than in the pre-lockdown period ( $884.5\text{ }\mu\text{g/L}$ ). The decrease of oxy-hydroxides by biodegradation of organic particles might explain the higher Fe content (Halim et al., 2010). Heavy toxic metals, e.g., Pb, have an average of  $67.8\text{ }\mu\text{g/L}$  and  $3.53\text{ }\mu\text{g/L}$  in both phases, respectively. Pre-lockdown mean values for Cd ( $33.7\text{ }\mu\text{g/L}$ ), Cr ( $161.3\text{ }\mu\text{g/L}$ ), Ni ( $146.7\text{ }\mu\text{g/L}$ ) and the post-lockdown mean values for Cd ( $0.097\text{ }\mu\text{g/L}$ ), Cr ( $6.91\text{ }\mu\text{g/L}$ ), Ni ( $11.56\text{ }\mu\text{g/L}$ ) in post lockdown. The trends of heavy metal concentrations in the pre-lockdown of water samples were  $\text{Fe} > \text{Zn} > \text{Cr} > \text{Cu} > \text{Ni} > \text{Mn} > \text{Pb} > \text{As} > \text{Cd}$  and in the post-lockdown the trend was  $\text{Fe} > \text{Mn} > \text{As} > \text{Zn} > \text{Ni} > \text{Cr} > \text{Cu} > \text{Pb} > \text{Cd}$ . The spatial distribution maps of the heavy metal(loid)s (Mn, Ni, Cu, Zn, Pb, Cd, Cr, As), that describe the variations in concentration levels between the two periods are shown in Fig. 3. Interestingly, during the post-lockdown period, Ni, Mn, and As concentrations were slightly high at the upper reach of the river (Fig. 3), which might be due to the intensive use of arsenical pesticides on the agricultural fields, accidental spills of Ni-containing items, municipal waste, rock, and soil weathering or extraction of other geological materials from the earth, and discharges of untreated waste. The high concentration of Ni, Mn, and As in the study area after the lockdown could have been caused by the lockdown or any of the other things listed above. The presence of settling mechanisms capable of transporting such metal(loid)s to shallow water layers and Holocene unconsolidated sediment could explain why surface water samples contain higher concentrations of those metal(loid)s (Proshad et al., 2022). According to Ravenscroft et al. (2005), the Holocene sediment is the primary host of As-contaminated groundwater in the study area. As contaminated groundwater is found in sediments from the Holocene along the channels of the Koratoya River, which is the main river in the study area.

In the current study, the observed concentrations of heavy metals in surface water during the pre-lockdown period were found to be higher than the values of heavy metals in surface water reported by Islam et al. (2021), where Islam et al. (2021) found  $49.5, 97.7, 78.4, 72.2, 51.5, 1.2, 105.7$  and  $21.2\text{ }\mu\text{g/L}$  for Mn, Ni, Cu, Zn, Pb, Cd, Cr and As, respectively; indicating that the concentrations of these heavy metals are increasing alarmingly in the surface water of the Karatoya River, which may pose toxic health hazards upon consumption. Heavy metal concentrations in water samples of the current study were matched to other relevant studies at the international levels, and unexpectedly, heavy metal values were clearly higher than the rivers of Meriç-Ergene River, Turkey (Tokatlı and Varol, 2021) and Zarjoub River, Iran (Haghnazar et al., 2022) (Table 3). Compared to several drinking water quality criteria, it was shown that As, Cd, Pb, Cr, Ni, Cu, Mn and Zn concentrations ( $\mu\text{g/L}$ ) in water samples were significantly greater than drinking water standard board (DWSB-0.05, 0.005, 0.05, 0.05, 100, 1.0, 0.1 and 5, respectively) (DoE (Department of Environment and Government of the People's Republic of Bangladesh), 1997); WHO-0.01, 0.003, 0.01, 0.05, 70, 2, 0.5 and 3, respectively (WHO, 2011); maximum contaminant level goal (MCLG-0.01, 0.005, 0.015 and 0.1 for As, Cd, Pb, and Cr) (USEPA, 2021) in water samples. The use of arsenical pesticides on the agricultural fields, chromate copper arsenate application on wood for wood processing, burning of coal for energy, leakage of sewage from the urban runoff (Kabir et al., 2020), and sediment excavation of the entire system of the study river (Islam, 2021). The rapid increase in heavy metal concentrations in the river water during the pre-lockdown period might be directly related to the extensive anthropogenic interventions like brick manufacturing, dredging, power production, metal emission from industries, galvanizing, refining, sludge disposal, and energy production (Shammi et al., 2022; Islam et al., 2022). Surprisingly, most of the metal levels decreased during the post-lockdown period. This



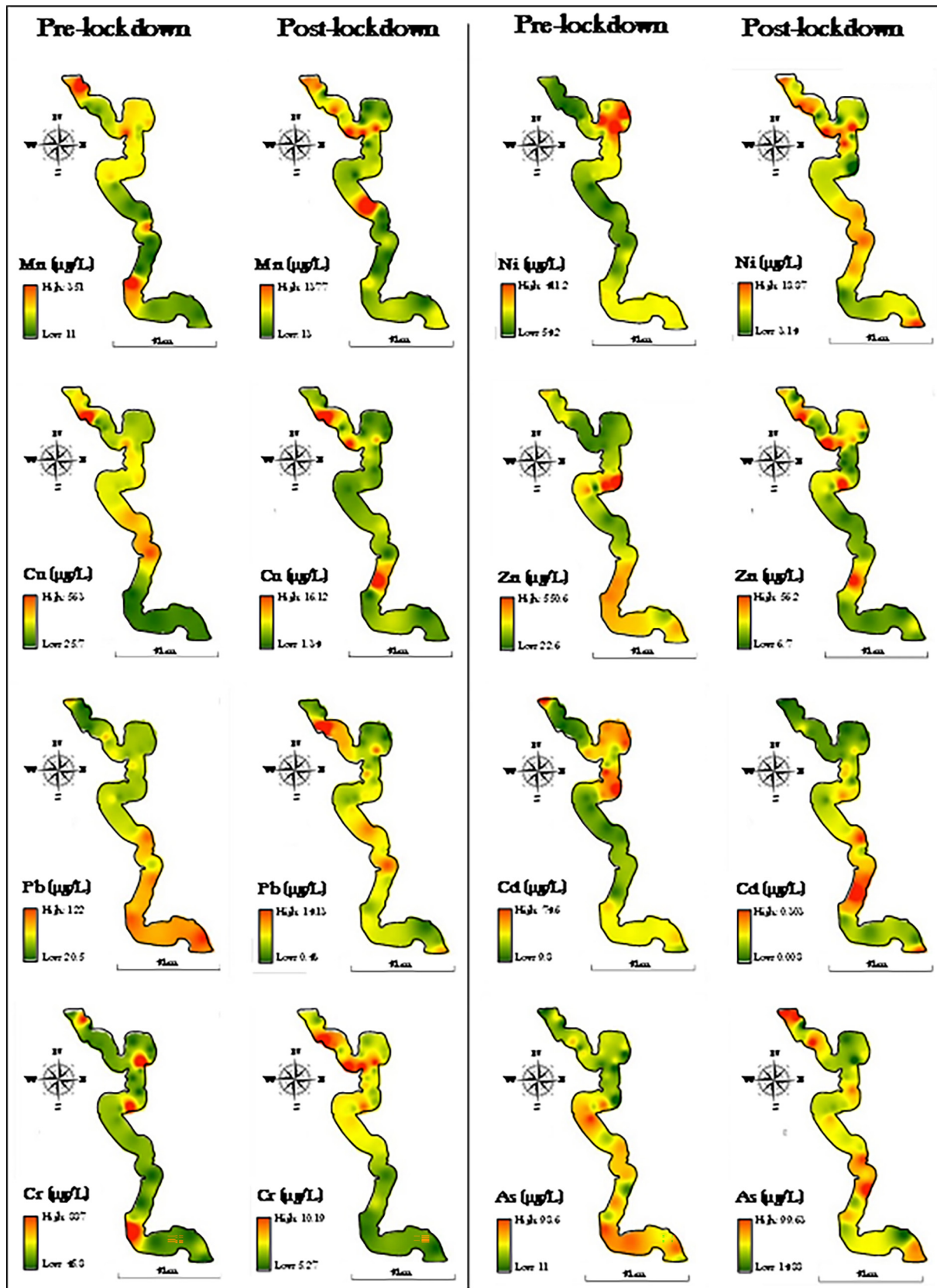


Fig. 3. Spatial distribution of heavy metal(loid)s during pre- and post-lockdown periods in the Karatoya River (Bangladesh).

might be due to the lockdown effect on the lower operations of various industries in the study area and other activities related to releasing heavy metals into the river water. However, concentrations of heavy metals

were lower during the post-lockdown period than in the pre-lockdown period in the surface water of the Meriç-Ergene River, Turkey (Tokatlı and Varol, 2021) and Zarjoub River, Iran (Haghnazar et al., 2022).

**Table 3**

Heavy metal concentration of surface water in pre- and post-lockdown periods in Karatoya River (Bangladesh) compared with other studies.

River →	Karatoya River, Bangladesh		Meriç-Ergene River, Turkey		Zarjoub River, Iran	
References →	This study		Tokatlı and Varol (2021)		Haghnazar et al. (2022)	
Metals/Period	Pre-lockdown	Post-lockdown	Pre-lockdown	Post-lockdown	Pre-lockdown	Post-lockdown
Mn	118.9 (11–351)	366.5 (13–1377)	26.3 (0.08–348.0)	28.01 (0.04–377.6)	–	–
Ni	146.7 (54.2–411.2)	11.56 (3.14–18.87)	9.06 (1.96–38.7)	0.97 (0.19–3.45)	21 (18–26)	31 (29–31)
Cu	154.5 (25.7–563)	3.87 (16.12–1.34)	4.30 (0.17–22.78)	0.71 (0.09–2.95)	5.20 (4–6.30)	1.10 (0.70–1.30)
Zn	181.4 (22.6–550.6)	19.4 (6.7–56.2)	8.18 (2.19–35.87)	1.29 (0.78–3.03)	29 (24–36)	39 (38–43)
Pb	67.78 (20.5–122)	3.53 (0.43–14.13)	0.51 (0.22–1.33)	0.15 (0.09–0.75)	15 (14–16)	14 (14–15)
Cd	33.71 (9.8–74.6)	0.10 (0.01–0.30)	0.05 (0.01–0.21)	0.02 (0.01–0.29)	–	–
Cr	161.3 (45.8–887)	6.91 (5.27–10.19)	13.76 (0.08–168)	0.83 (0.03–13.16)	56 (44–72)	24 (15–32)
As	55.23 (11–98.6)	58.07 (14.88–99.63)	3.51 (0.12–17.35)	1.40 (0.20–4.03)	3.20 (3–3.60)	3.60 (2.60–4.60)

According to Fig. 3, the concentration of Pb showed that a higher level of Pb mainly contaminated the southeastern part of the river in the pre-lockdown periods. This might be happening due to the urban pollution and industrial influences on that area (Haghnazar et al., 2022). The pollution level fell after the COVID-19 lockdown due to the limitation on industrial activity during the lockdown. Furthermore, a higher contamination level of Cd was observed in the northeastern part of the river basin during the pre-lockdown phase. The overall contamination, including the north-east, was reduced in the post-lockdown phase. This happened because of the river basin's limited human and industrial activity during the COVID-19 lockdown (Patel et al., 2020). In the case of As concentration, the middle and the southeastern parts of the river basin were contaminated mainly by As during the pre-lockdown periods. However, after the lockdown, the concentration of As increased overall, with the northwestern and southeastern parts showing the highest contamination of As. Though the other heavy metal(loid)s were reduced during the lockdown, contamination did not decline as expected. This might be happening because the concentration of river water depends upon diverse sources like geological and anthropogenic ones (Dutta et al., 2020).

### 3.2. Assessment of heavy metal(loid)s pollution indices

The HPI values varied from 212.5 to 898.8 with a mean value of 596.1 for all the surface samples collected in the pre-lockdown phase. In contrast, during the post-lockdown phase, they ranged from 53.94 to 338.9 with a mean value of 178.6 (Fig. 4A). According to these results, the HPI values exceeded the highest acceptable index value of 100 in both phases. Though the HPI values at all sampling sites decreased in the post-lockdown periods, they are still above the permissible limit. The highest reduction was recorded at sampling site 31 due to the limited industrial inputs during the lockdown. In contrast, sampling site 4 had the lowest reduction amount of HPI value due to agricultural overflow and effluent discharge from the drainage system. The spatial distribution of HPI in both periods is shown in Fig. 5A–B. The spatial distribution of HPI evaluated the high and low pollution areas in both phases. The spatial distribution of HPI indicated that the north and the south parts of the river basin were highly polluted in the pre-lockdown periods (Fig. 5A). The northeastern and the southwestern parts of the river were moderately polluted during the pre-lockdown phase. The polluted area was dominated by industrial activities, waste dumping, and agricultural practices (Custodio et al., 2021). On the other hand, in the post-lockdown phase, the northern and northwestern parts of the river basin were mainly polluted (Fig. 5B). This happened due to domestic waste dumping and limited industrial activities in those areas during the lockdown. However, the overall pollution was reduced after the COVID-19 pandemic (Shukla et al., 2021).

The results of the HEI indicated that, during the pre-lockdown period, all the samples varied from 12.44 to 49.42 with an average value of 31.30, while in the post-lockdown, they varied from 4.03 to 69.04 with an average value of 23.81 (Table S6). All of the HEIs were higher than the highest acceptable value of 10, which means that heavy metal(loid)s polluted all the sampling sites before the lockdown. The HEI values decreased during the lockdown in sampling sites 03, 10, 12, 16, 21, and 33,

indicating lower pollution in that area than in pre-lockdown periods (Fig. 4B). At sampling site 31, the amount of reduction was the highest. At sampling site 1, the amount of decline was the lowest. On the other hand, sampling site 05 has the highest rate of pollution in the post-lockdown compared with the pre-lockdown phase. That might have happened due to domestic waste dumping in the river. The HEI findings showed a substantial enhancement in overall surface water quality during the post-lockdown (Fig. 5C–D). Further, the HEI indicated that the southwestern part of the river basin was more polluted than the other parts during the pre-lockdown periods (Fig. 5C). Industrial activity was higher in this part. But in the post-lockdown periods, pollution was reduced in the southwestern part. A higher level of pollution was seen in the north-western part of the river basin (Fig. 5D). After the lockdown, the level of pollution in that area mainly rose because people dumped their trash there (Selvam et al., 2020).

The NPI values in the pre-lockdown period ranged from 1.81 to 12.87, with a mean value of 6.80 for all the sampling sites. During the post-lockdown period, they had a range of 0.42 to 20.18, with a mean value of 4.99 (Table S6). According to NPI, sampling site 07 has the highest rate of decrease in pollution level and shows the clarity of the water (<1). On the other hand, sampling site 05 has an increased pollution level (>7) in the post-lockdown period and shows highly polluted water in that area (Fig. 4C). This may have happened due to the area's household waste and agricultural activity. The NPI indicates that, overall, the water is moderately polluted ( $2.5 < PN \leq 7$ ) in both phases. The HPI, HEI, and NPI results showed a significant drop in heavy metal pollution and a big improvement in the overall quality of the river water post-lockdown.

The spatial distribution of Nemerow's pollution index (NPI) in the pre-lockdown periods demonstrated that the northern and northeastern parts of the basin had the highest level of NPI value (Fig. 5E). But in the post-lockdown periods, the overall pollution level decreased according to the NPI index (Fig. 5F). However, some areas located in the northwestern part of the river basin had the highest level of pollution during the post-lockdown periods. This might have happened due to increased waste disposal sites in that part of the river basin (Proshad et al., 2022).

### 3.3. Source of heavy metals (loids) and factors influencing river water quality

After the dataset was collected using the centered log-transformed method, PC/FA was used to find the links between elements, differences in Euclidean space, and possible sources of the geochemical association. The KMO scores (0.519 and 0.596) and Bartlett's test of sphericity values ( $p < 0.001$ ) indicated that the surface water data from the pre-and post-lockdown periods were suitable for PC/FA analysis. Except for modifying the coordinate system of the physicochemical elements, the commonality approach was linked with varimax rotation, which was utilized to check the PC/FA and provide a fundamental expression of these elements. In the distribution of metal sources, PC is a viable statistical method (Kumar et al., 2021). Concurrently, multivariate outliers were removed from the river water datasets since the existence of outliers may cause bias in the analysis's outcomes (Reimann et al., 2012; Buccianti and Grunsky, 2014; Filzmoser et al., 2018; Pawlowsky-Glahn et al., 2015; Herms et al., 2021).

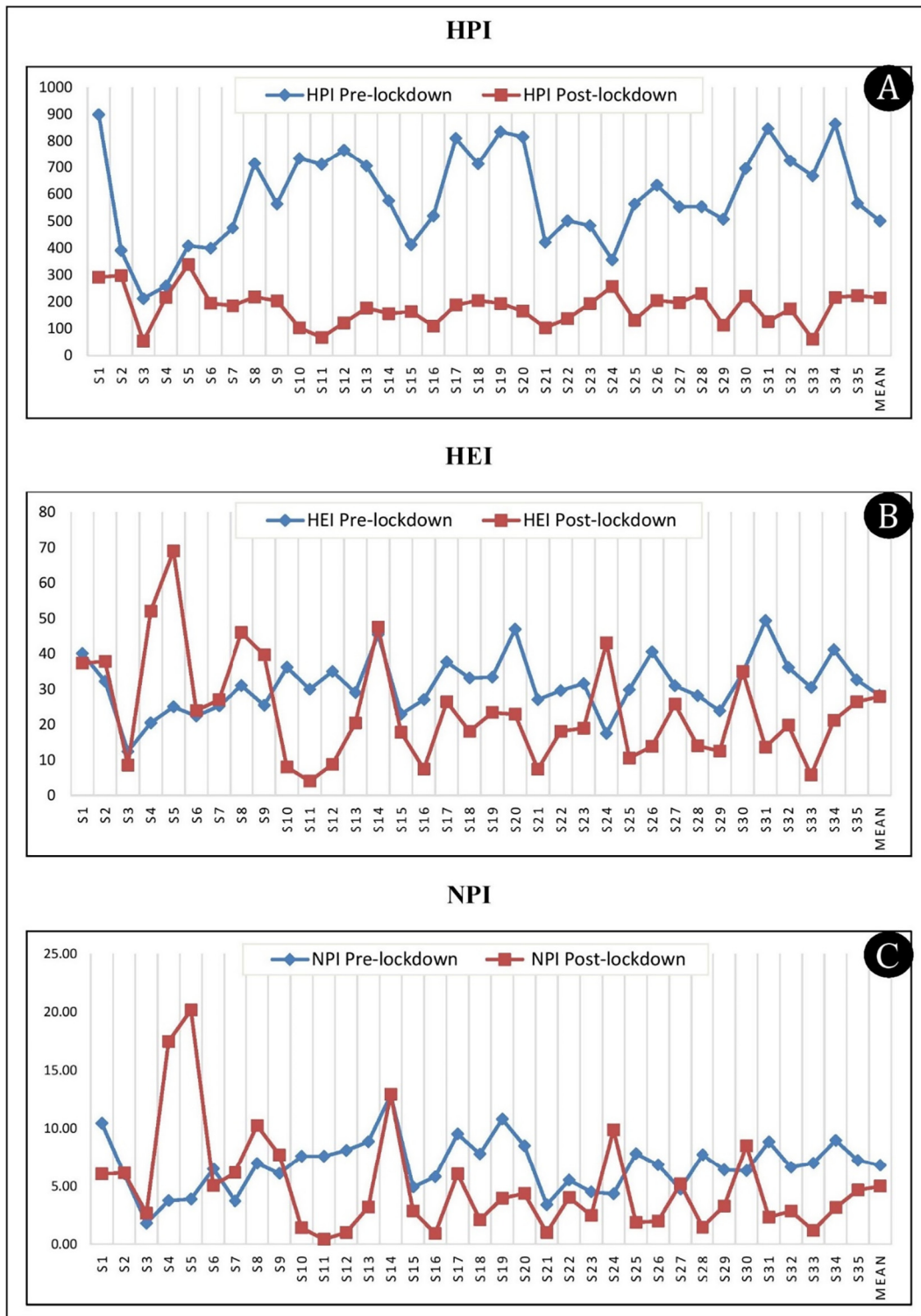


Fig. 4. Spatial-temporal variations of (A) heavy metals pollution index (HPI), (B) heavy metals evaluation index (HEI), and (C) Nemerow's pollution index (NPI) in Karatoya River (Bangladesh).

Overall, three variables were picked based on the 1-mark break-point of the scree-plot, which account for 46.86 % and 60.96 % of the dataset variability in river water, respectively (Fig. S1). The extracted components for the river water observed for pre-lockdown were PC1, PC2, and PC3, as responsible for 19.11 %, 16.24 %, and 10.88 % of the data variability, respectively. Similarly, the three components found for the post-lockdown dataset, PC1, PC2, and PC3, account for 35.98 %, 15.15 %, and 11.70 %, respectively, of the data variability (Table S7).

It is critical to recognize the categories of components descending side by side and the weight of their loading as the biplot of the CLR-transformed data. The pH ( $r = 0.713$ ), Ca ( $r = 0.818$ ), Ni ( $r = 0.701$ ), and Cd ( $r = 0.768$ ) loadings of the initial PC1 were all highly positive (Fig. 6A and B). Higher Ni and Cd readings indicate contamination from anthropogenic sources such as wastewater discharge from houses and industrial effluents, which account for water pollution (Kumar et al., 2022). The second component PC2 showed substantial positive loadings for Na



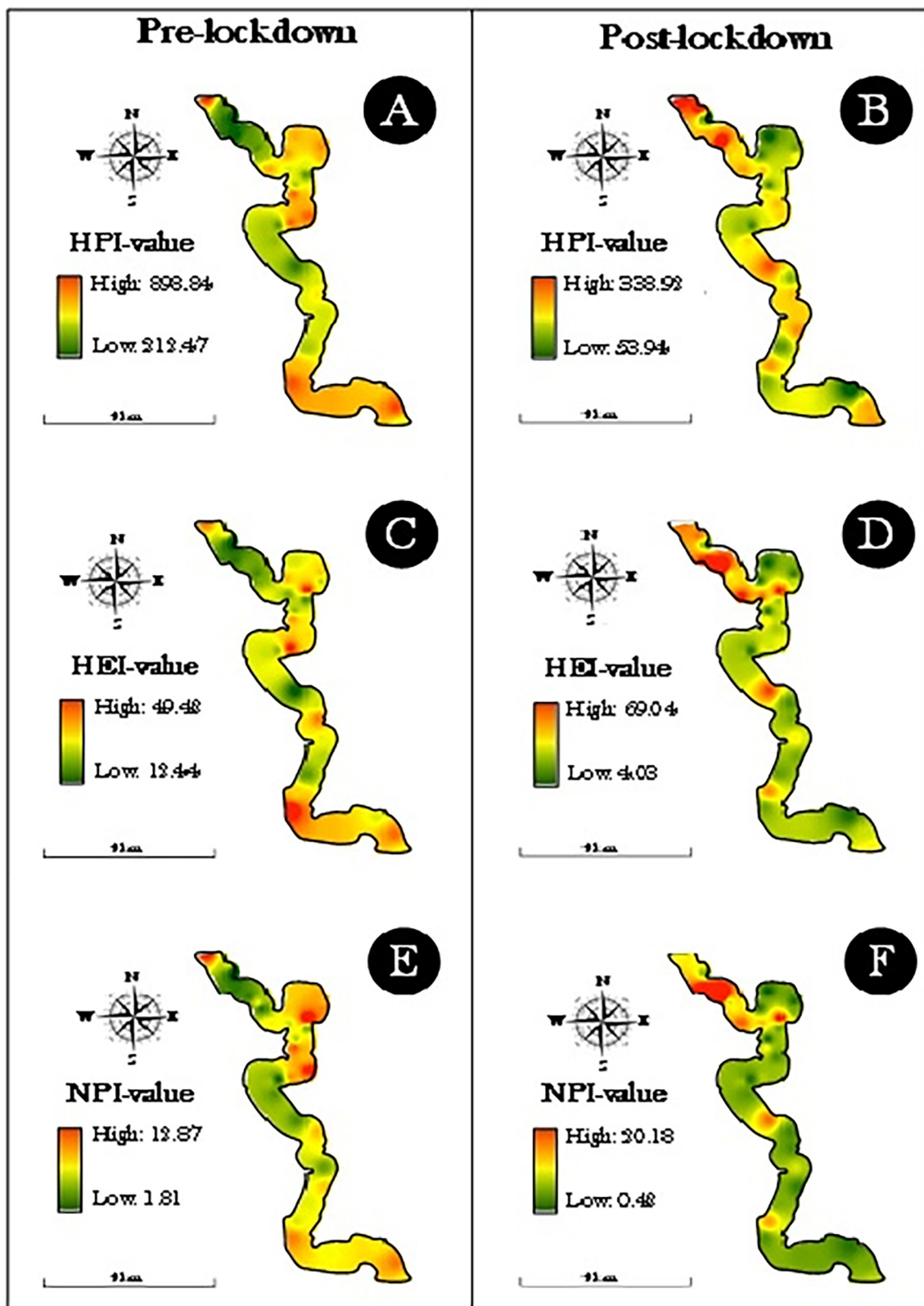


Fig. 5. Spatial distribution of (A) heavy metals pollution index (HPI), (B) heavy metals evaluation index (HEI), and (C) Nemerow's pollution index (NPI) in pre- and post-lockdown periods, Karatoya River (Bangladesh).

( $r = 0.863$ ), Mg ( $r = 0.901$ ), and Pb ( $r = 0.646$ ), showing that industrial activities in the river basin are the primary source of these metals in river water (Dokmeci, 2017; Islam, 2021; Tokatlı and Varol, 2021). DO ( $r = 0.827$ ) and Zn ( $r = 0.802$ ) were strongly positively loaded by the third

PC3. Zn is mostly introduced into water by artificial activities such as coal combustion, steel manufacture, or waste material combustion (Habib et al., 2020). These metals' origins might be related to small-scale industrial activity. Their concentrations rise during the rainy season owing to surface



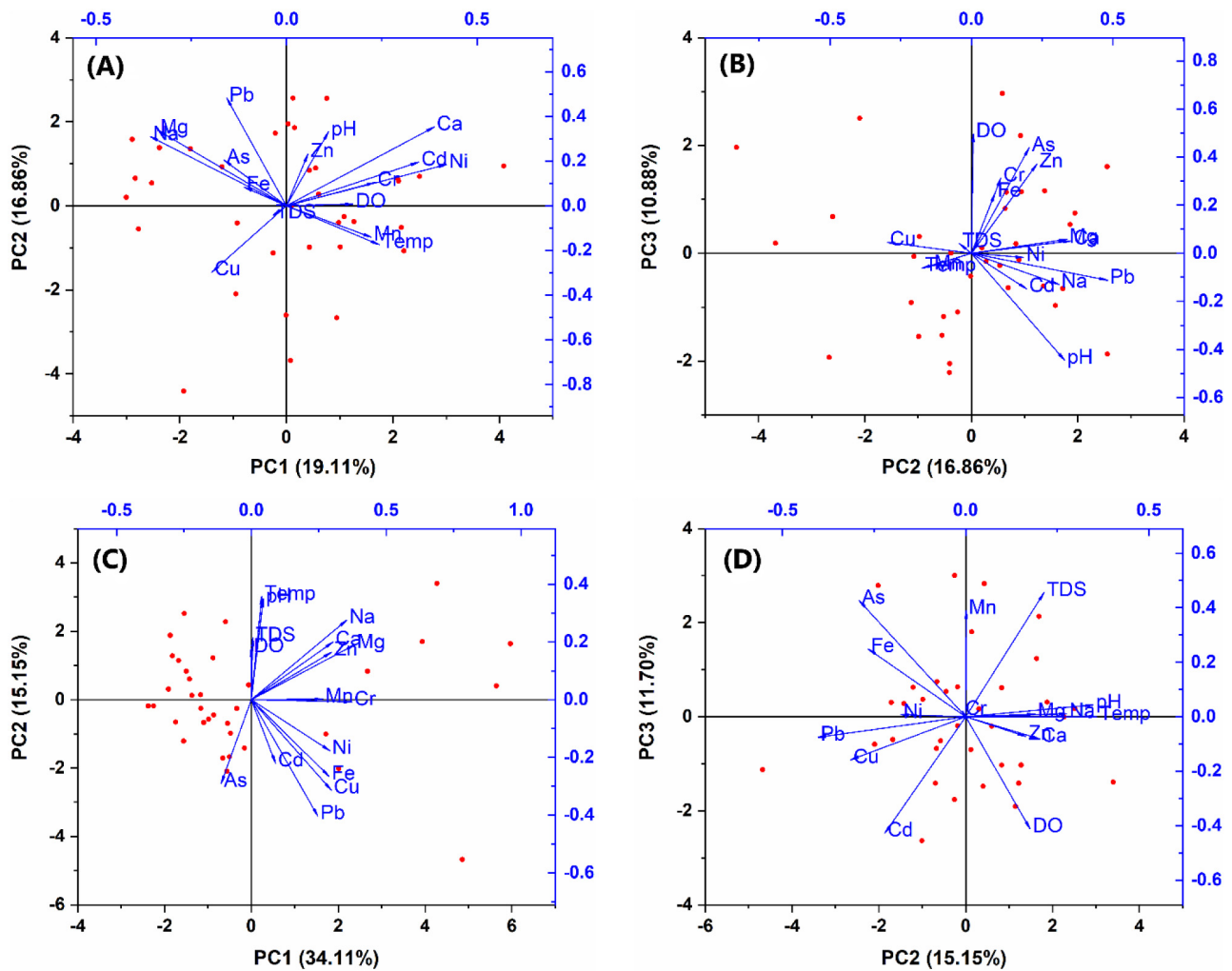


Fig. 6. Multivariate statistics representation of river water samples in the Karatoya River during the pre-lockdown and post-lockdown phase (a) Biplot of factor 1 vs 2; (b) Biplot of factor 2 vs 3 in pre-lockdown; (c) Biplot of factor 1 vs 2 (d) Biplot of factor 2 vs 3 in post-lockdown phase.

runoff and anthropogenic loadings, such as municipal and industrial waste emissions (Islam et al., 2020). According to Table S7, both Ni and Cd in river water have higher PC1 loadings, suggesting that they arise from diverse sources of pollution. Lead input into aquatic water originates from urban waste leachates, including nickel-cadmium batteries from vehicle workshops, scrapping of Pb from batteries, smelting facilities, and other sources (Fig. 6B) (Wu et al., 2009; Shammii et al., 2022). This occurs daily in the study region around the sugar mill as a hot dumping point for their wastewater runoff. Our findings are consistent with surface water contamination in other parts of the world (Kumar et al., 2021). In short, the PC/FA could point to three main sources of heavy metal(oids) pollution in river water: industrial emissions, point sources, and non-point sources.

We noticed a clear trend in pre-lockdown principal component PC1 from the post-lockdown dataset that was identical to PC1 from the pre-lockdown dataset (Fig. 6C and D). The PC1 of the post-lockdown period showed significant positive loadings on Na ( $r = 0.894$ ), Mg ( $r = 0.873$ ), Ca ( $r = 0.895$ ), and Zn ( $r = 0.576$ ). The sources of these components, which did not decrease over the lockdown period, include organic substances and household wastewater outflow (Khan et al., 2021a). Strong positive loadings on Fe ( $r = 0.862$ ), Ni ( $r = 0.569$ ), Cu ( $r = 0.805$ ), Pb ( $r = 0.829$ ), and Cr ( $r = 0.734$ ) were shown by the second component PC2. The high values of Fe, Cu, Ni, and Pb in this PC2 suggest artificial sources of pollution such as agricultural runoff, home waste disposal, and effluents from industrial plants that may have had to function throughout the lockdown period (Tokatl and Varol, 2021; Proshad et al., 2022). In PC3, DO ( $r = 0.804$ ) has a significant positive loading. This might be

attributed to a decrease in pollutants and an improvement in overall river water quality after the lockout (Chakraborty et al., 2022). The main source of Ni and Cu in surface water bodies is phosphate-based fertilizers used on agricultural land (Qu et al., 2018; Islam et al., 2022). Lead is mostly emitted through fossil fuels, car tires, oil leaks, and roadside dust (Kumar et al., 2022). The runoff from the city may be a viable route for these contaminants into river water bodies. Overall, the PC/FA showed that heavy metal(oid)s pollution in water comes from two main sources: man-made and natural.

The Pearson correlation coefficient (PCI) of these 16 variables is carried out to quantify the relationships among the pairs of attributes that influence the surface water quality in both phases. The analyzed results of the PCI with the correlation coefficients are displayed in Fig. 7. The analogous source of contaminants coming into the surface water bodies from the same pathways is identified by the high correlations detected among the investigated attributes (Bhardwaj et al., 2017; Varol, 2019). According to the PCI, Cr significantly correlates with Ca and Ni. Significant correlations were determined between Cd, pH, Ca, and Ni. The significant positive correlation demonstrates a link between the same sources of contamination (natural or caused by humans) and their mobility (Haloi and Sarma, 2012). Pb had a positive association with pH, Na, and Mg. DO and Zn had only a significant correlation. Cu had a strong negative correlation with Ca and Pb in the pre-lockdown phase. Mg and Na had a strong inverse relationship.

On the other hand, in the post-lockdown period, Cr showed a significant positive association with most of the metals except for Cd. Cd had a negative correlation with TDS and a positive correlation with Cu. Pb showed a

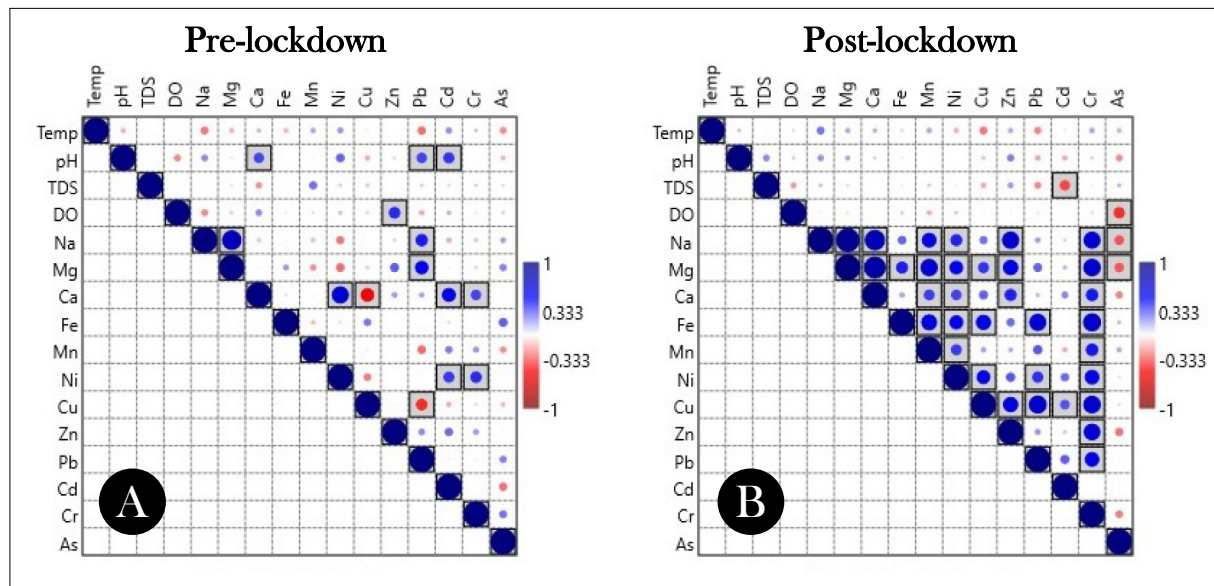


Fig. 7. Pearson's correlation matrix among the measured attributes in (A) pre-lockdown and (B) post-lockdown periods evaluated in Karatoya River (Bangladesh).

strong positive association with Fe and Cu. Zn had similar concentrations to Na, Mg, and Cu. Ni had a moderate positive correlation with all other variables. Ca-Na-Mg had a significant correlation with each other. As it had a similar negative correlation with DO, Na, and Mg. Applied PCI results also denoted the presence of insignificant correlations in other elements. This finding indicates the independent sources of these attributes (Kamrani et al., 2016).

HCA was employed to find the relationship between the metal(loid) concentrations and probable sources. Moreover, similar groups of sampling sites can be represented along with the distinct groups by employing cluster analysis (Hossain et al., 2021). The findings of the HCA indicated that industrial activities mostly dominated the Karatoya River basin, so a separate cluster with elevated contamination levels was formed in the pre-lockdown. But in the post-lockdown period, it has been part of the "more contaminated zone". Overall water quality improved during the post-lockdown, according to the findings of CA2 (post-lockdown period). But, the number of relatively contaminated sites increased in the post-lockdown phase. The surface water quality of the Karatoya basin, which received extreme industrial pressure, generally decreased the impacts significantly in the lockdown period. However, the outcomes of the HCA demonstrated that, during the post-lockdown period, they had sustained participation in the "Relatively More Contaminated Zone" clustering site. This cluster was subjected to domestic pollution during the lockdown. Therefore, the sampling sites in the post-lockdown were grouped into the "Relatively More Contaminated Zone" cluster than in the pre-lockdown phase.

Similar findings were found by Tokatlı and Varol (2021), who found that the contaminated zone increased in the cross-boundary river basin in Turkey during the post-lockdown phase. This may have occurred due to the lack of waste management facilities during the lockdown, so people dumped their domestic waste in the surrounding river basin area. During the continuous lockdown, people stay home all the time, so domestic waste increases more than in previous times. This also increases the contaminated zone during the lockdown. If the post-lockdown data of some significant locations in the basin were compared with the pre-lockdown data set of those locations, substantial reductions in toxic element concentrations were recorded in river water. The cluster analysis of investigated attributes during pre-and post-lockdown was shown in Fig. 8. The PCA results were supported by the fact that there were clusters among the study sites. This showed that most of the metals came from human actions, such as chemical fertilization, industrial waste, raw materials from homes and farms, and so on.

River water quality is controlled by several natural and anthropogenic factors, including the climatic regime (temperature and rainfall), river regime, changes in land use and land cover (LULC), and land management practices in a river basin (Sarkar et al., 2021b). Natural driving forces act long-term, while anthropogenic activities induce rapid, short-term changes in water quality (Sarkar and Islam, 2020). In the present study, we observed the rainfall pattern, river discharge, and evapotranspiration at Bogra station in the KRB, Bangladesh, and basin LULC during the pre-lock-down phases (March to May 2019) and post-lock-down phases (March to May 2022) to depict the influence of the various natural and anthropogenic forces on the river water quality (Table 4). The study found that in the pre-lock-down phases, monthly average rainfall ranged from 2 mm to 144 mm. In the post-lock-down phase, on the other hand, it ranged from 4 mm to 91 mm. There was no significant difference between the pre-and post-phases, as shown by the computed *F* value is lower than the tabulated value (0.207) and the *p*-value being higher (0.693).

Similarly, river discharge fluctuated from 486 cusecs to 938 cusecs in the pre-lock down phases. In comparison, it ranged from 343 cusecs to 691 with no significant difference between the pre and post-lock-down phases (*F*: 0.810, *p*: 0.463). Moreover, evapotranspiration showed no significant difference (*F*: 5.776, *p*: 0.138). The LULC during this short period did not change much, mainly due to the COVID pandemic. Thus, the radical fall in the concentration of the pollutants, especially the heavy metals in the post-lock-down phases, is undoubtedly due to the COVID-19 pandemic, the principal cause of the change inducer. Heavy metal pollution is mainly triggered by anthropogenic influxes, which came to a minimum during and immediately after the COVID-19 pandemic.

### 3.4. Health risk assessment

Based on the health risk evaluation model suggested by the USEPA, the carcinogenic and non-carcinogenic risks to personal health via ingestion and dermal pathways of the heavy metals (loids) in surface water from the study basin were calculated. Daily consumption of Cr, As, Cd, Pb, Mn, Ni, Cu, and Zn via contaminated river water over pre-and post-lockdown phases was assessed for both age groups. The results of HQ (ingestion), HQ (dermal), and HI results are summarized in Table S8. According to the guidelines given by the USEPA (US Environmental Protection Agency) (2009), the safe level recommended for a non-cancer hazard quotient (HQ) is 1.00 for all heavy metals. Regarding the water through the oral pathway, As, Cd, and Mn during the pre-lockdown period had the highest HQ values for adults and children (Table S8), while in the post-lockdown

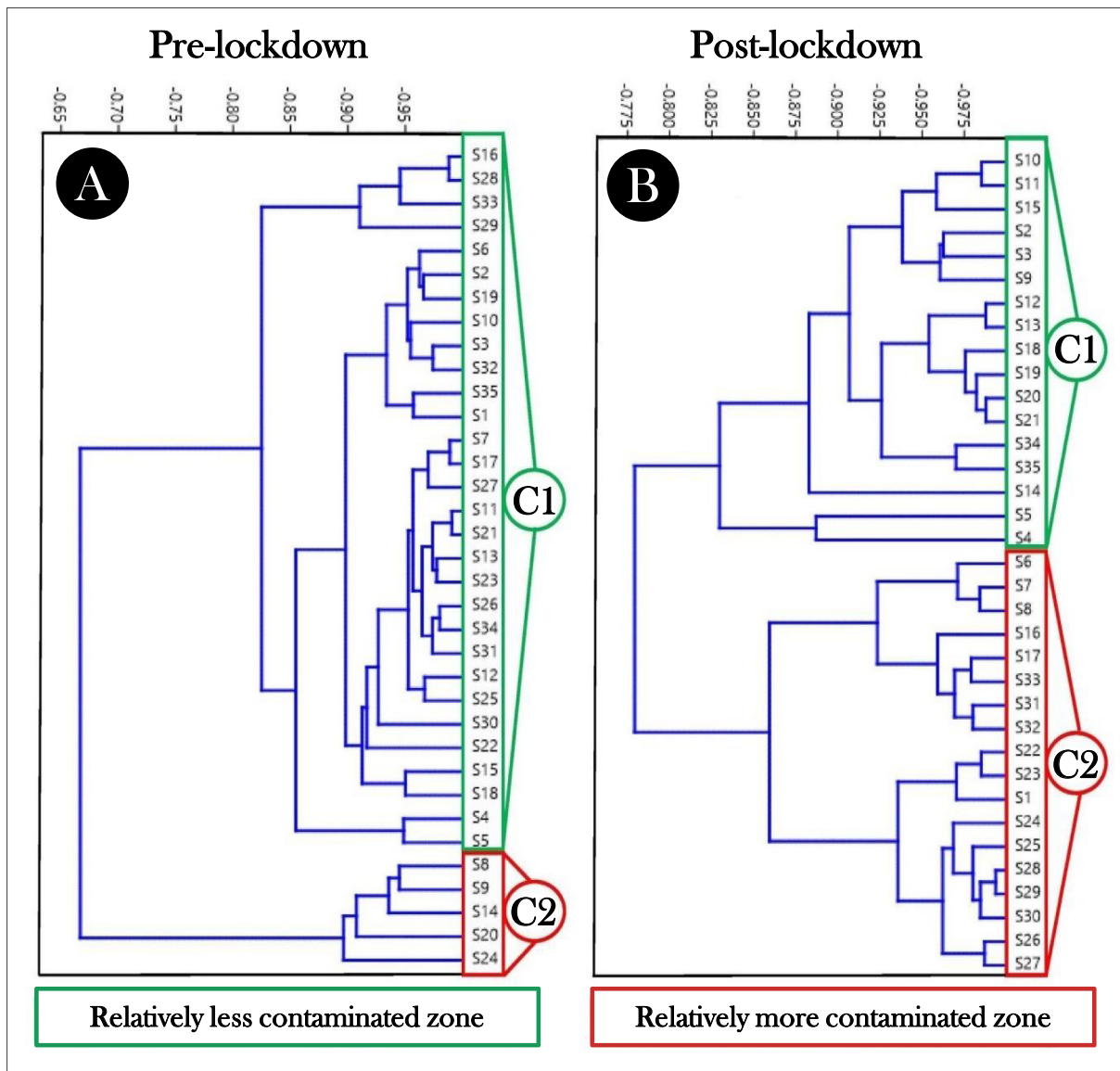


Fig. 8. Dendrograms of the hierarchical cluster analysis (CA) of the sampling sites for the (A) pre-lockdown and (B) post-lockdown in Karatoya River (Bangladesh).

period, As and Mn had the highest HQ values. In the case of the dermal exposure pathway, As is the metal with the maximum HQ values for both age groups in the pre-lockdown, and Mn and As had the maximum HQ values in the post-lockdown (Table S8). The HQ values of all metals (loids) for both age groups via oral pathways in the pre-and post-lockdown phases were higher than the acceptable non-carcinogenic risk level of 1, except for Ni, Cu, and Zn. However, in the pre-and post-lockdown periods, HQ values for all metals in adults and children via dermal pathways were lower than the acceptable non-carcinogenic risk level (1). The HI values for the oral water pathway for both age groups were higher than the acceptable limit in the cases of Cr, As, Cd, Pb, and Mn in the pre-lockdown. But in the post-lockdown, the risk is minimized for both age populations, except for

**Table 4**  
Single way ANOVA showing the pre-post lockdown difference of the various drivers controlling the river water quality.

Parameters	F	P-value	F crit	Significance level	Remarks
Rainfall	0.207	0.693	18.512	0.05	Null
River Discharge	0.810	0.463	18.512	0.05	Null
Evapotranspiration	5.776	0.138	18.512	0.05	Null

As and Mn (Fig. 9). There are many possible routes of human exposure to As and Mn from both natural and anthropogenic sources, as it is a common metal in nature. Arsenic is the 20th most prevalent element in the Earth's crust (Cullen and Reimer, 1989; Henke, 2009), and it may be found in over 240 distinct minerals, the most frequent of which being sulfides, sulfosalts, arsenates, and arsenites, the arsenic-containing minerals (Thornton and Farago, 2012). Humans can also cause contamination. Arsenic is extensively utilized in manufacturing alloys, batteries, glass, insecticides, textiles, and wood preservation (Gilhotra et al., 2018). According to Table S8, the trend for non-carcinogenic risks, according to the HI value of heavy metals (loids) for adults, is As > Mn > Cd > Cr > Pb in pre-lockdown and As > Mn in post-lockdown phases. The non-carcinogenic risk trend for children is As > Mn > Cd > Cr > Pb and in the post-lockdown phase, Mn > As.

In our study, the CR values of Cr, As, Cd, and Pb for both age populations in the pre-lockdown were higher than the tolerable carcinogenic risk range of 10–6 to 10–4, the limit set by the US EPA (2004). However, in the post-lockdown period, only the CR values of As for both adults and children were higher than the acceptable limit (Fig. 10). In terms of age, children have a higher CR than adults in both pre-and post-lockdown phases. This may happen because the consumption rate and exposure are

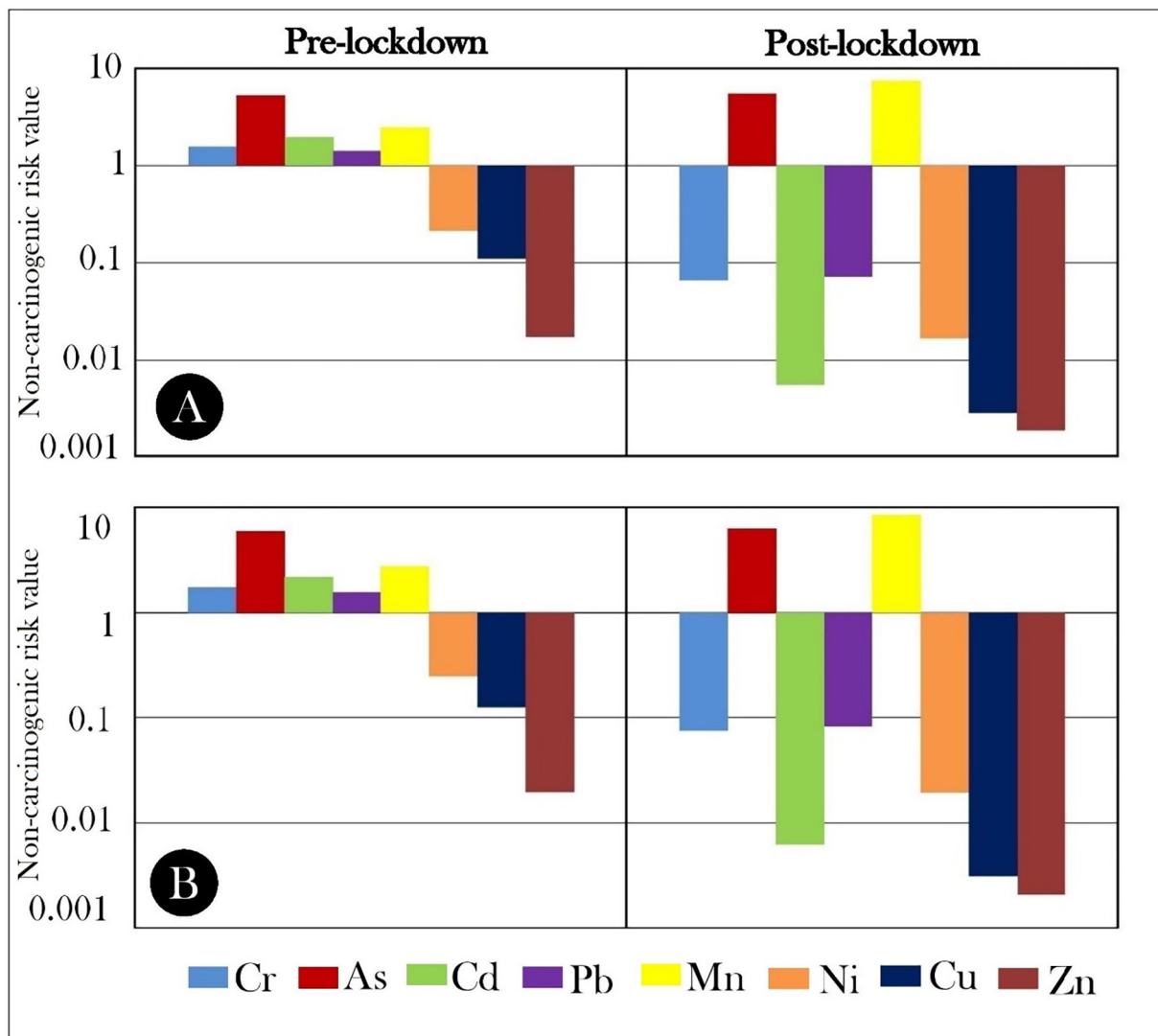


Fig. 9. Non-carcinogenic risks of heavy metal(loid)s for (A) adults and (B) children in pre- and post-lockdown periods in Karatoya River (Bangladesh).

higher for children. In the health risk assessment, As was the primary contaminant to human health, particularly for children (Xiao et al., 2019). So, the increase in heavy metal (loids) pollution in the surface water mostly harms children, which can be ignored. The abundance of As in river water can depend on for various reasons. Natural, residential, industrial, and electronic waste, fly ash deposition, sewage discharge, and religious activities are all potential causes of arsenic pollution (Mahipal et al., 2018). The long-term monitoring program of As in river water and effective health education for As pollution are necessary. From the above discussions, it can be easily assumed that all the CR risks were reduced due to the lockdown.

### 3.5. Assessment of irrigation water quality during pre-lockdown and post-lockdown

The Karatoya River has substantially contributed to irrigation purposes for rural and urban Bogura district, Bangladesh. Salinity is a critical ecological factor in the survival of organisms (Islam et al., 2022). But excessive salt concentrations over the recommended range damage flora and animals (Pant et al., 2021). Potential salinity is more fluctuating near the shore than in inland water (Shil et al., 2019; Sarkar et al., 2021a). In this study, the SAR of the Karatoya River ranged from 2.70 to 8.87, with an average value of 5.58 in the pre-lockdown (Table S9). On the other hand, in the post-lockdown, the range was between 1.21 and 3.86, with an average of 1.82. Compared with the pre-lockdown, the SAR value reduction in the post-lockdown phases clearly shows the improvement in irrigational

water quality. The comparison of the two periods' SAR values is shown in Fig. 11A. Generally, near agricultural land, the SAR values are frequently high because of the failure of the soil's physical structure by various agricultural activities (Barik and Pattanayak, 2019).

The MR of the Karatoya River ranged between 6.78 and 22.15 and 14.29 to 24.20 in the pre- and post-lockdown phases, respectively. The pre-lockdown has a mean MR value of 13.80, and the post-lockdown has a mean value of 20.77. The MR values of the two periods are shown in Fig. 11B. Here, the MR value of the post-lockdown value increased more than during the post-lockdown period. A >50 % MR value indicates a high Mg concentration, while an MR value of <50 % represents a suitable concentration of Mg in irrigational uses (Sundaray et al., 2009). The higher MR value in the post-lockdown period may depend on natural processes.

On the other hand, KI values varied between 0.48 and 1.77, with an average value of 1.04 in the pre-lockdown period, whereas in post-lockdown, the average value was 0.43, with a range between 0.27 and 0.76. KI values for two periods are shown in Fig. 11C. According to Kelly's index, a KI value of less than one is suitable, while a KI value of >1 is unsuitable for irrigation purposes. The pre-lockdown crosses the standard value of 1 according to the KI. The post-lockdown value remains below 1, which indicates that irrigation water quality has improved during the lockdown due to the restriction on industrial activity and other human activities related to water pollution. The spatial distribution of SAR, MR, and KI is presented in Fig. 12.



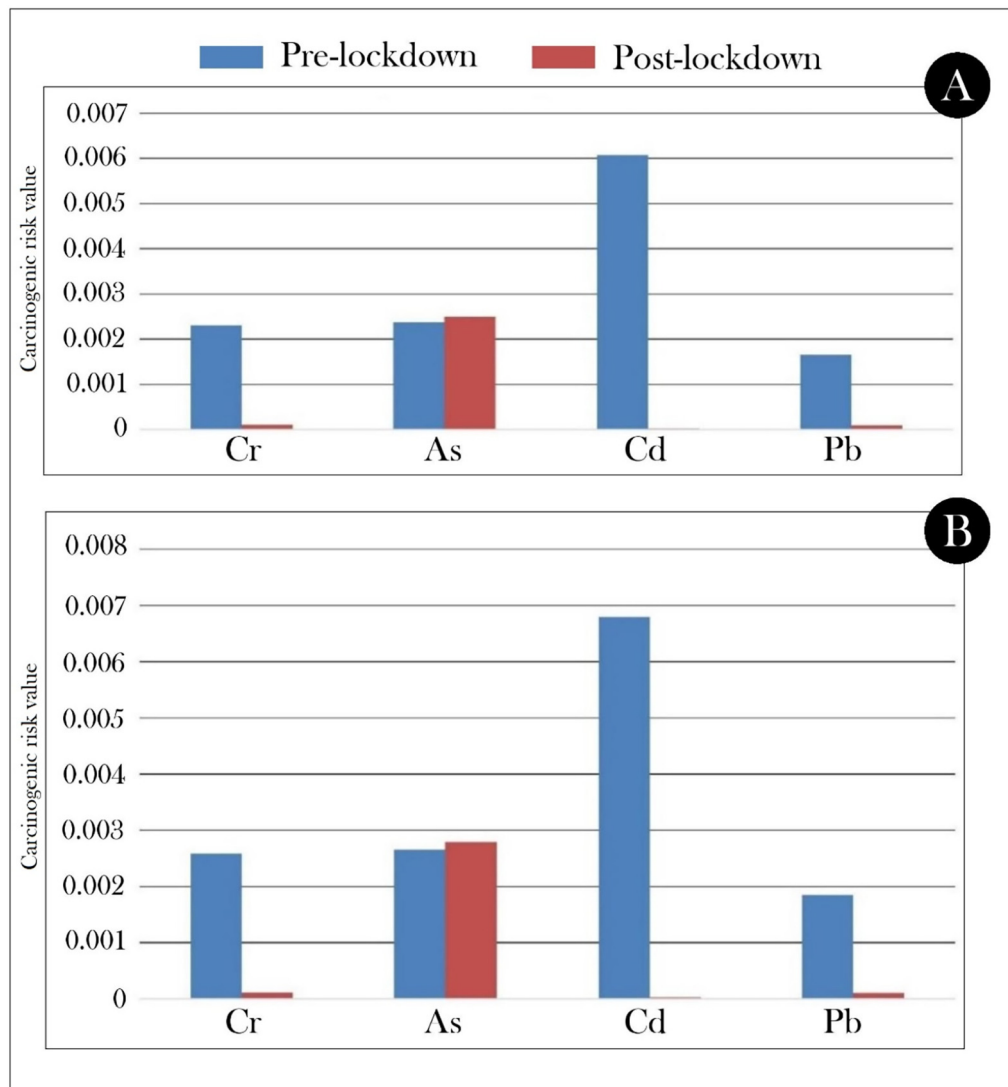


Fig. 10. Carcinogenic risks of heavy metal(loid)s for (A) adults and (B) children in pre-and post-lockdown periods in Karatoya River (Bangladesh).

The spatial distribution of sodium absorption ratio (SAR) demonstrated that the middle part of the river basin had the highest level of SAR value in the pre-lockdown periods (Fig. 12A). However, only a few areas in the northwestern part of the river basin had a higher level of SAR value after the lockdown (Fig. 12B). Industries like the tannery industries are the main sources of sodium in the river water (Islam et al., 2015).

Fig. 12C shows the spatial distribution of magnesium rate (MR) values in the pre-lockdown periods. The middle section of the river basin had the maximum MR value. On the other hand, during the post-lockdown overall, the MR value increased (Fig. 12D). The northeastern and middle parts of the river basin showed the highest levels of MR value in the post-lockdown periods. In Fig. 12E, Kelly's index (KI) values during pre-lockdown periods are evaluated. The results showed that the higher KI value was in the middle and the southwestern portions of the river basin. But during the post-lockdown periods, the high KI value was seen in the northeastern part of the river basin (Islam et al., 2017) (Fig. 12F).

### 3.6. Spatial variation of water quality indices and heavy metal (loids) using geostatistical modeling

The experimental semivariogram plots with error factors considered (ME, RMSE, MS, RMSS, and ASE) for the different distributions showed that Mn, Cu, Cd, Cr, As, HPI and HEI are best fitted using the OK model. In contrast, Ni and KI are fitted with the OK model, and Zn and Pb are fitted

with the IDW model in the pre-lockdown period (Table S10). But, all the chemical species and indices except for Cr are fitted with the SK model, while Cr is fitted with the IDW model post lockdown period (Table S11). Different theoretical semivariogram models are based on the smallest nugget value (Goovaerts, 1997). The elements such as nugget size, significant range (Km), sill size, lag size, and nugget/sill ratio of the pre-lockdown phase and post-lockdown phase are shown in Tables S12 and S13. Based on the nugget/sill ratio (NS), the spatial dependence of a distribution is determined. When the NS remains below 0.25, it denotes a strong spatial variation, while NS ranging from >0.25 to 0.75 implies moderate spatial dependence, and NS > 0.75 shows a weak spatial variation (Shi et al., 2007; Sarkar et al., 2021b). We found that in the pre-lockdown period, HPI, SAR, MR, and KI depicted strong spatial variations, while Mn showed a moderate variation, while others showed weak patterns (Table S12 and Fig. S2). However, we found mostly weak spatial dependence in the post-lockdown phases, except for a few moderate spatial variations for Cd, As, HPI, and KI. However, no chemical species or indices showed significant spatial variation after the lockdown period (Table S12). This may be due to the self-purification hydrochemical processes in the wake of COVID-19 and the related lower fluxes of the effluents discharged from the urban and industrial belts of the KRB. Moreover, in the pre-lockdown period, Mn, Cd, AS, HPI, HEI, MR, and KI showed the best fit with the circular model of the kriging technique, while Zn and Pb showed the best fit with the power equation of the IDW model (Table S12). The spherical model

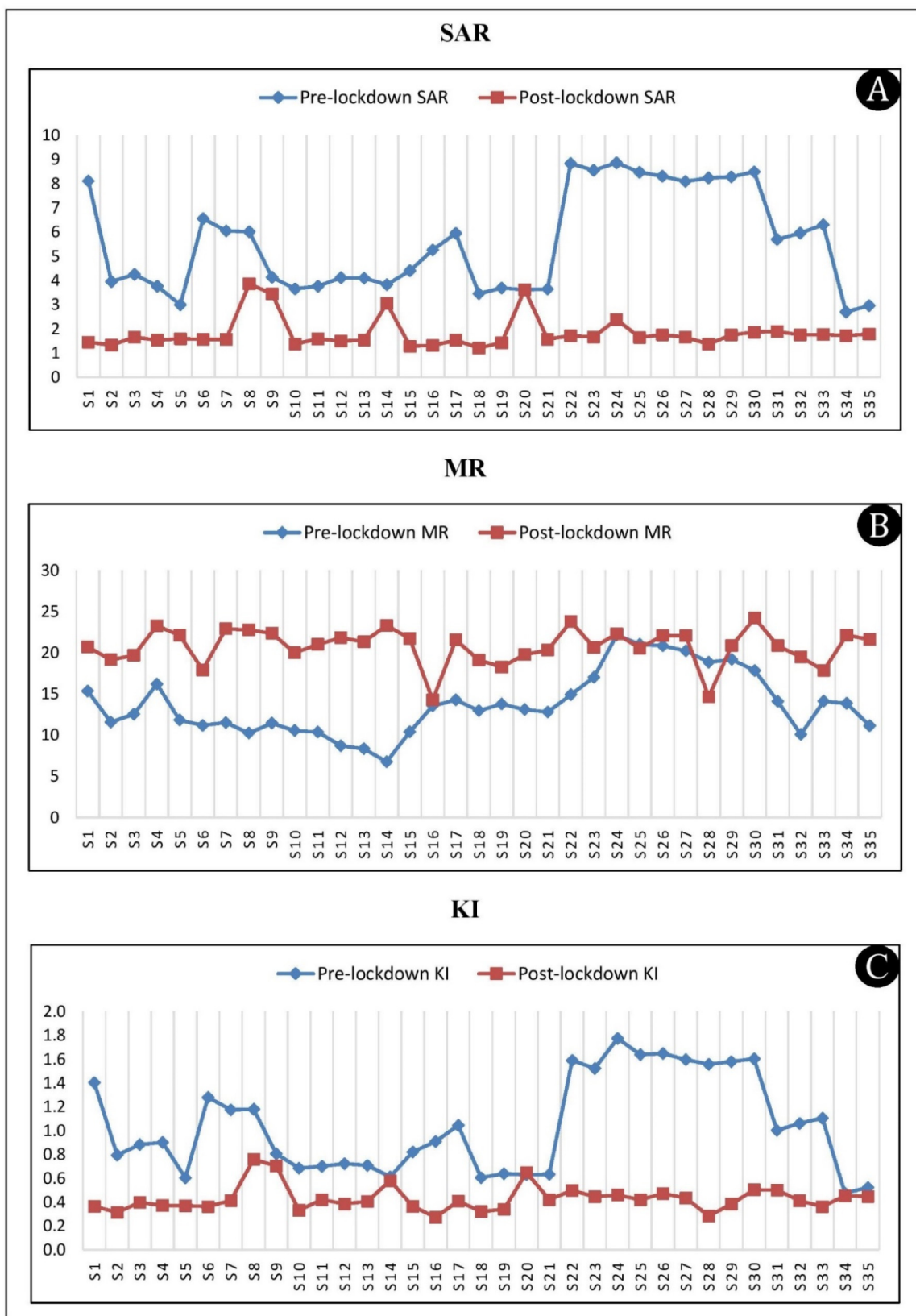


Fig. 11. (A) Sodium absorption ratio (SAR), (B) magnesium rate (MR), and (C) Kelly's index (KI) values for water samples in pre- and post-lockdown periods in Karatoya River (Bangladesh).

fits best for Ni and Cr, while the Gaussian model fits best for Cu and the exponential model fits best for SAR (Table S12). Besides, in the post lockdown period, Mn, NI, HPI, and KI showed the best fit with the spherical model,

Cu, Pb, As, HEI, and MR with the circular model, and Zn and SAR with the exponential model under the kriging technique, while Cr was best fitted with the power equation (Table S13 and Fig. S3). In general, kriging

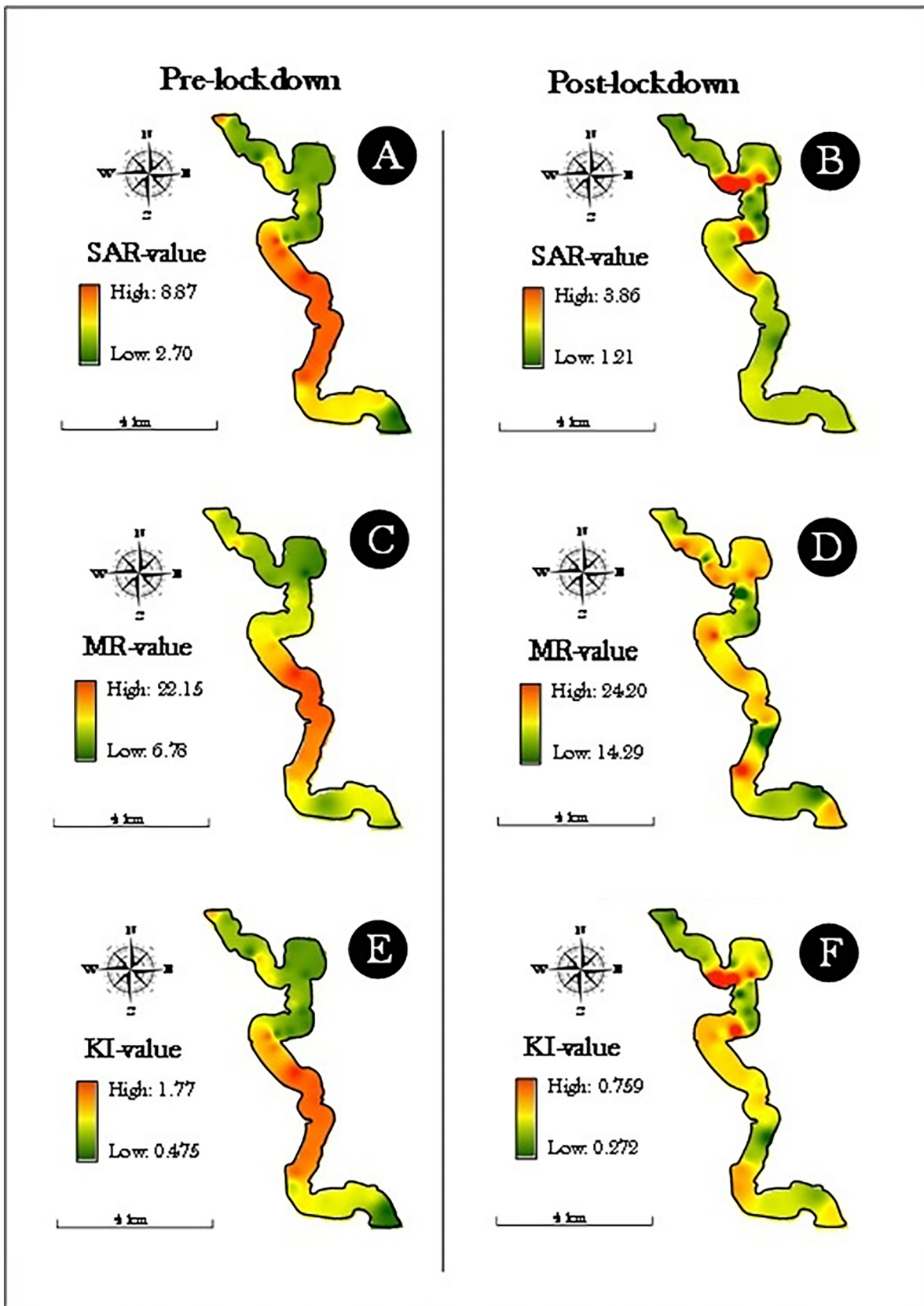


Fig. 12. Spatial distribution of (A-B) sodium absorption ratio (SAR), (C-D) magnesium rate (MR), and (E-F) Kelly's index (KI) values in pre- and post-lockdown periods in Karatoya River (Bangladesh).

techniques were found to be more suitable for showing most distributions, except for Zn and Pb in the pre-lockdown period and Cr in the post-lockdown period. This could be because the data structures are different, i.e., datasets with more changes may be better shown with IDW (Sarkar et al., 2021a).

### 3.7. Policy implications for sustainable eco-restoration strategies

The study's results may be valuable to academics, policymakers, and stakeholders for long-term surface water management and recovering contaminated river systems. Further study is needed to ensure the safety of the water in the KRB and to enhance its quality. It will be implemented in the development project that will be helpful to the assessment of surface water quality in Bangladesh. The outcomes will provide information on water quality status and preliminary human health safety. They can also be used as a set of surface water quality data in Bangladesh for further comparisons. Investigating the effects of the COVID-19 lockdown on heavy metal pollution of water and the associated health risk assessment is a small step. Key lessons from the COVID-19 pandemic for river management include addressing industrial effluents and providing sufficient flow releases. The four key lockdown suggestions are important lessons for future eco-restoration.

- Strict quality control and enforcement are needed to check wastewater treatment and discharge noncompliance. National pollution control boards may need to address this issue. Existing industries require third-party environmental compliance verification to increase efficiency and transparency.
- Before returning the wastewater to the study river, it must be treated. Industrial pollution in Karatoya contributes roughly 30 % by volume, but its toxicity and high inorganic impurities impact the aquatic ecology more. The industries satisfy the norms and compliance, yet pollution is considerable in the post-covid period. In light of this, the mandated criteria should be revised.
- Several water abstraction and drainage projects on the Karatoya River were planned without considering its ecological demands. Excessive water abstraction and pollution reduce aquatic life and a river's ability to self-purify and dilute. It seems that river flow rules were designed exclusively for water; sediment movement, biota, and nutrients were overlooked. Therefore, a comprehensive flow regime of suitable amplitude, timing, frequency, and duration is needed to support aquatic ecosystems.
- Untreated and partly treated hazardous industrial waste from tanneries, mills, factories, electroplating, and distilleries is the primary source of water pollution in the middle part of the basin. Therefore, a relentless effort is needed to reduce pollution from hotspots.

## 4. Conclusions

This is the first research in Bangladesh to examine the imprints of the lockdown on the river water quality and preliminary health risk in the Karatoya River Basin (KRB) concerning COVID-19s unprecedented impacts. The results showed a noteworthy reduction in water pollution and associated carcinogenic health risk in the KRB during the lockdown period compared to the pre-lockdown phase, demonstrating clear spatio-temporal variations caused primarily by some restrictions on industrial activities and the reduction of direct industrial effluents during the lockdown period. In contrast, water pollution increased in the middle portion of the river basin, thus deteriorating water quality because of ongoing anthropogenic activities. The non-carcinogenic health risks of heavy metal (loid)s rise to some extent due to the increase in Fe, Mn, and As concentrations during the lockdown. The CDA results confirmed that the water quality in the KRB is affected by a direct discharge of untreated industrial effluents, agricultural runoff, solid waste, and traffic pollution in the pre-lockdown period. In contrast, it is influenced by weathering, disinfection byproducts, municipal wastewater, and lockdown effect for the lower operation of various industries during the post-lockdown period. Similarly, the

irrigation water quality of the KRB was identified as a safe limit in both pre-and post-lockdowns, with significant improvement in water quality after lockdown. We found no significant differences in the climatic regime (temperature and rainfall), river regime, changes in LULC, and land management practices in a river basin during pre-to-post phases ( $p > 0.05$ ). The circular semivariogram models have been verified as the best fit models in the pre-lockdown phase. In contrast, the spherical semivariogram models showed the optimal model for most of the water quality indices and heavy metal(loid)s during the post lockdown period. We also found that HPI, SAR, MR, and KI depicted strong spatial variations in the pre-lockdown period, while in the post-lockdown phase, river water quality indices have weak spatial patterns except for Cd, As, HPI and KI. However, degrading water quality, particularly in the mid-central part of the river, could cause severe problems for crop production in the study area, where river water is the only source of irrigation. Thus, the COVID-19 lockdown served as a ventilator, allowing the KRB's water quality to improve.

Overall, the rapid recovery of a heavily contaminated river basin is only feasible with little human intervention. A further comprehensive investigation is necessary to ensure this basin's river water safety and security. Given the rising pace of urbanization and pollution loading in the river, essential measures should be implemented to minimize future degradation of river water quality. The issue would be to retain the river in comparable conditions after the lockdown, which could be achieved with a twofold increase in current treatment facilities, strict industrial pollution control measures, and behavioral changes to enhance infrastructure building.

### CRedit authorship contribution statement

**Jawad-Ul-Haque:** Methodology, Investigation, Sample collections and preparation. **Aznarul Islam, and Md. Abu Bakar Siddique** Methodology, Validation. **Abu Reza Md. Towfiqul Islam:** Conceptualization, Writing - original draft preparation, Writing - reviewing and editing, Supervision. **Md. Saiful Islam and Cem Tokatli:** Sample analysis, Data curation and interpretation, Writing - reviewing and editing. **Subodh Chandra Pal and Abubakr M. Idris:** Original draft preparation, Reviewing and editing. **Guilherme Malafaia, and Mir Mohammad Ali:** Reviewing and editing. All authors read and approved the final manuscript.

### Funding

The authors extend their appreciation to the Deanship of Scientific Research at King Khalid University for funding this work through Small Groups Project under grant number (RGP.1/215/43).

### Data availability

Data will be made available on request.

### Declaration of competing interest

The authors declare that they have no known competing financial interests or personal relationships that could have appeared to influence the work reported in this paper.

### Acknowledgements

The authors thank the National Council for Scientific and Technological Development (CNPq/Brazil) for granting of research productivity grant to Dr. Malafaia G. (proc. #308854/2021-7).

### Appendix A. Supplementary data

Supplementary data to this article can be found online at <https://doi.org/10.1016/j.scitotenv.2022.159383>.



## References

- Ahsan, M.A., Satter, F., Siddique, M.A.B., Akbor, M.A., Ahmed, S., Shajahan, M., Khan, R., 2019. Chemical and physicochemical characterization of effluents from the tanning and textile industries in Bangladesh with multivariate statistical approach. *Environ. Monit. Assess.* 191 (9), 1–24. <https://doi.org/10.1007/s10661-019-7654-2>.
- Ali, H., Yilmaz, G., Fareed, Z., Shahzad, F., Ahmad, M., 2020. Impact of novel coronavirus (COVID-19) on daily routines and air environment: evidence from Turkey. *Air Qual. Atmos. Health* <https://doi.org/10.1007/s11869-020-00943-2>.
- Aman, A.A., Salman, M.S., Yunus, A.P., 2020. COVID-19 and its impact on the environment: improved pollution levels during the lockdown period – a case from Ahmedabad, India. *Remote Sens. Appl. Soc. Environ.* 20, 100382.
- Aman, M.A., Salman, M.S., Ali, P.Y., 2020. COVID-19 and its impact on environment: improved pollution levels during the lockdown period—a case from Ahmedabad, India. *Remote Sens. Appl. Soc. Environ.* 100382. <https://doi.org/10.1016/j.rsase.2020.100382>.
- Arif, M., Kumar, R., Parveen, S., 2020. Reduction in Water Pollution in Yamuna River Due to Lockdown Under COVID-19 Pandemic. 22. *ChemRxiv*, pp. 3389–3406.
- Aydın, S., Nakiyingi, B.A., Esmen, C., Güneysu, S., Ejjada, M., 2020. Environmental impact of coronavirus (COVID-19) from Turkish perspective. *Environ. Dev. Sustain.* <https://doi.org/10.1007/s10668-020-00933-5>.
- Bangladesh Bureau of Statistics (BBS), 2020. *Yearbook of Agricultural Statistics of Bangladesh, 2020*. Bangladesh Bureau of Statistics, Dhaka.
- Bao, R., Zhang, A., 2020. Does lockdown reduce air pollution? Evidence from 44 cities in northern China. *Sci. Total Environ.* 731, 139052.
- Barik, R., Pattanayak, S.K., 2019. Assessment of groundwater quality for irrigation of green spaces in the Rourkela city of Odisha, India. *Groundw. Sustain. Dev.* 8, 428–438. <https://doi.org/10.1016/j.gsd.2019.01.005>.
- Bhardwaj, R., Gupta, A., Garg, J.K., 2017. Evaluation of heavy metal contamination using environmental and indexing approach for River Yamuna, Delhi stretch, India. *WaterSci.* 31, 52e66.
- Bodrud-Doza, M., Shammi, M., Bahlman, L., Islam, A.R.M.T., Rahman, M.M., 2020. Psychosocial and socio-economic crisis in Bangladesh due to COVID-19 pandemic: a perception-based assessment. *Front. Public Health* 8, 341. <https://doi.org/10.3389/fpubh.2020.00341>.
- Bortey-Sam, N., Nakayama, S.M.M., Ikenaka, Y., Akoto, O., Baidoo, E., Mizukawa, H., Ishizuka, M., 2015. Health risk assessment of heavy metals and metalloids in drinking water from communities near gold mines in Tarkwa Ghana. *Environ. Monit. Assess.* 187, 397. <https://doi.org/10.1007/s10661-015-4630-3>.
- Buccianti, A., Grunsky, E., 2014. Compositional data analysis in geochemistry: are we sure to see what really occurs during natural processes? *J. Geochem. Explor.* 141, 1–5. <https://doi.org/10.1016/j.jexplo.2014.03.022>.
- Chakraborty, B., Roy, S., Bera, A., Adhikary, P.P., Bera, B., Sengupta, D., Bhunia, G.S., Shit, P.K., 2021. Cleaning the river Damodar (India): impact of COVID-19 lockdown on water quality and future rejuvenation strategies. *Environ. Dev. Sustain.* <https://doi.org/10.1007/s10668-020-01152-8>.
- Chakraborty, B., Bera, B., Adhikary, P.P., Bhattacharjee, S., Roy, S., Saha, S., Sengupta, D., Shit, P.K., 2022. Effects of COVID-19 lockdown and unlock on the health of tropical large river with associated human health risk. *Environ. Sci. Pollut. Res.* <https://doi.org/10.1007/s11356-021-17881-w>.
- Chaurasia, S., Singh, R., Tripathi, I.P., Ahmad, I., 2020. Imprints of COVID -19 pandemic lockdown on water quality of river Mandakini, Chitrakoot, Satna (M.P. IJSDR 5 (10), 275–281.
- Chen, R., Zhang, Q., Chen, H., Yue, W., Teng, Y., 2021. Source apportionment of heavy metals in sediments and soils in an interconnected river-soil system based on a composite fingerprint screening approach. *J. Hazard. Mater.* 411, 125125.
- UN Water, United Nation, 2018. *Sustainable Development Goal 6 (SDG-6), Synthesis Report on Water and Sanitation (Accessed 21 December, 2021)*.
- Collivignarelli, M.C., Abba, A., Bertanza, G., Perazzani, R., Ricciardi, P., Miio, M.C., 2020. Lockdown for CoViD-2019 in Milan: what are the effects on air quality? *Sci. Total Environ.* 732, 139280.
- Cullen, W.R., Reimer, K.J., 1989. Arsenic speciation in the environment. *Chem. Rev.* 89, 713–764. <https://doi.org/10.1021/cr00094a002>.
- Custodio, M., Peñaloza, R., Alvarado, J., Chanamé, F., Maldonado, E., 2021. Surface water quality in the Mantaro River watershed assessed after the cessation of anthropogenic activities due to the COVID-19 pandemic. *Pol. J. Environ. Stud.* 30 (4), 3005–3018.
- Dantas, G., Siciliano, B., França, B.B., da Silva, C.M., Arbilla, G., 2020. The impact of COVID-19 partial lockdown on the air quality of the city of Rio de Janeiro, Brazil. *Sci. Total Environ.* 729, 139085.
- Dash, S., Borah, S.S., Kalamdhad, A.S., 2021. Heavy metal pollution and potential ecological risk assessment for surficial sediments of Deepor Beel, India. *Ecol. Indic.* 122, 107265.
- DoE (Department of Environment, Government of the People's Republic of Bangladesh), 1997. *ECR (The Environment Conservation Rules)*, pp. 179–226. Poribesh Bhaban E-16, Agargaon, Shere Bangla Nagar Dhaka 1207, Bangladesh.
- Dokmeci, A.H., 2017. Evaluation of heavy metal pollution in the Ergene River Basin from a public health perspective. *Turk. J. Public Health* 15, 212–221.
- DPHE (Department of Public Health Engineering), 2001. *Arsenic Contamination of Groundwater in Bangladesh, 2. Final Report*. British Geological Survey, Keyworth, UK.
- Dutta, V., Dubey, D., Kumar, S., 2020. Cleaning the River Ganga: impact of lockdown on water quality and future implications on river rejuvenation strategies. *Sci. Total Environ.* 743, 140756.
- Duttagupta, S., Bhanja, S.N., Dutta, A., Sarkar, S., Chakraborty, M., Ghosh, A., Mondal, D., Mukherjee, A., 2021. Impact of Covid-19 lockdown on availability of drinking water in the arsenic-affected Ganges River Basin. *Int. J. Environ. Res. Public Health* 18, 2832. <https://doi.org/10.3390/ijerph18062832>.
- Edet, A.E., Offiong, O.E., 2002. Evaluation of water quality pollution indices for heavy metal contamination monitoring. A study case from Akpabuyo-Odukpani area, Lower Cross River Basin (southeastern Nigeria). *GeoJournal* 5, 295–304.
- Filzmoser, P., Hron, K., Templ, M., 2018. *Applied Compositional Data Analysis. With Worked Examples in R*. Springer Series in Statistics <https://doi.org/10.1007/978-3-319-96422-5>.
- Ge, Y., Lou, Y., Xu, M., Wu, C., Meng, J., Shi, L., Xia, F., Xu, Y., 2021. Spatial distribution and influencing factors on the variation of bacterial communities in an urban river sediment. *Environ. Pollut.* 272, 115984.
- Ghanbarpour, M.R., Goorazi, M., Vahabzade, G., 2013. Spatial variability of heavy metals in surficial sediments: Tajan River Watershed, Iran. *Sustain. Water Qual. Ecol.* 1–2, 48–58.
- Gilhotra, V., Das, L., Sharma, A., et al., 2018. Electrocoagulation technology for high strength arsenic wastewater: process optimization and mechanistic study. *J. Clean. Prod.* 198, 693–703. <https://doi.org/10.1016/j.jclepro.2018.07.023>.
- Goovaerts, P., 1997. *Geostatistics for Natural Resource Evaluation*. Oxford University Press, New York.
- Goovaerts, P., 2000. Geostatistical approaches for incorporating elevation into the spatial interpolation of rainfall. *J. Hydrol.* 228, 113–129.
- Habib, M.A., Islam, A.R.M.T., et al., Bodrud-Doza, 2020. Simultaneous appraisals of pathway and probable health risk associated with trace metals contamination in groundwater from Barapukuria coal basin, Bangladesh. *Chemosphere* 242, 125183. <https://doi.org/10.1016/j.chemosphere.2019.125183>.
- Haghnazar, H., Cunningham, J.A., Kumar, V., Aghayani, E., Mehraein, M., 2022. COVID-19 and urban rivers: effects of lockdown period on surface water pollution and quality- a case study of the Zarjoub River, north of Iran. *Environ. Sci. Pollut. Res.* <https://doi.org/10.1007/s11356-021-18286-5>.
- Halim, M.A., Majumder, R.K., Nessa, S.A., Oda, K., Hiroshiro, Y., Jinno, K., 2010. Arsenic in shallow aquifer in the eastern region of Bangladesh: insights from principal component analysis of groundwater compositions. *Environ. Monit. Assess.* 61, 453–472. <https://doi.org/10.1007/s10661-009-0760-9>.
- Halo, N., Sarma, H.P., 2012. Heavy metal contaminations in the groundwater of Brahmaputra flood plain: an assessment of water quality in Barpeta District, Assam (India). *Environ. Monit. Assess.* 184 (10), 6229–6237.
- Hasanuzzaman, M., Song, X., Han, D., Zhang, Y., Hussain, S., 2017. Prediction of groundwater dynamics for sustainable water resource management in Bogra district, Northwest Bangladesh. *Water* 9, 238. <https://doi.org/10.3390/w9040238>.
- Hasanuzzaman, M., Song, X., Han, D., Zhang, Y., Hussain, S., 2017. Prediction of groundwater dynamics for sustainable water resource management in Bogra District, Northwest Bangladesh. *Water* 9, 238. <https://doi.org/10.3390/w9040238>.
- Hem, J.D., 1991. *Study and Interpretation of the Chemical Characteristics of Natural Waters*. 3rd edn. Scientific Publishers, Jodhpur Book 2254.
- Henke, K.R., 2009. Arsenic in natural environments. In: Henke, K.R. (Ed.), *Arsenic-Environmental Chemistry, Health Threats and Waste Treatment*. Wiley, Chichester, pp. 69–236.
- Hermis, I., Jódar, J., Soler, A., Lambán, L.J., Custodio, E., Núñez, J.A., Arnó, G., Ortego, M.I., Parcerisa, D., Jorge, J., 2021. Evaluation of natural background levels of high mountain karst aquifers in complex hydrogeological settings. A Gaussian mixture model approach in the Port del Comte (SE, Pyrenees) case study. *Sci. Total Environ.* 756, 143864. <https://doi.org/10.1016/j.scitotenv.2020.143864>.
- Hossain, M.B., Semme, S.A., Ahmed, A.S.S., Hossain, M., Porag, G.S., Parvin, A., Sekar, S., 2021. Contamination levels and ecological risk of heavy metals in sediments from the tidal river Halda, Bangladesh. *Arab. J. Geosci.* 14 (3), 1–12.
- Hu, K., Li, B., Lu, Y., Zhang, F., 2004. Comparison of various spatial interpolation methods for non-stationary regional soil mercury content. *Environ. Sci.* 25 (3), 132–137.
- Islam, A.R.M.T., Shen, S., Bodrud-Doza, M.D., Rahman, M.S., 2017. Assessing irrigation water quality in Faridpur district of Bangladesh using several indices and statistical approaches. *Arab. J. Geosci.* 10 (19), 418.
- Islam, A.R.M.T., Mamun, A.A., Rahman, M.M., Zahid, A., 2020. Simultaneous comparison of modified-integrated water quality and entropy weighted indices: implication for safe drinking water in the coastal region of Bangladesh. *Ecol. Indic.* 113, 106229. <https://doi.org/10.1016/j.ecolind.2020.106229>.
- Islam, A.R.M.T., Pal, S.C., Chakraborty, R., Idris, A.M., Salam, R., Islam, M.S., Shahid, S., Zahid, A., Ismail, Z.B., 2022. A coupled novel framework for assessing vulnerability of water resources using hydrochemical analysis and data-driven models. *J. Clean. Prod.* 336 (6), 130407. <https://doi.org/10.1016/j.jclepro.2022.130407>.
- Islam, M.S., 2021. Preliminary assessment of trace elements in surface and deep waters of an urban river (Korotoa) in Bangladesh and associated health risk. *Environ. Sci. Pollut. Res.* 28, 29287–29303. <https://doi.org/10.1007/s11356-021-12541-5>.
- Islam, M.S., Ahmed, M.K., Raknuzzaman, M., Habibullah-Al-Mamun, M., Islam, M.K., 2015. Heavy metal pollution in surface water and sediment: a preliminary assessment of an urban river in a developing country. *Ecol. Indic.* 48, 282–291.
- Islam, M.S., Idris, A.M., Islam, A.M.R.T., Phoungthong, K., Ali, M.M., Kabir, M.H., 2021. Geochemical variation and contamination level of potentially toxic elements in land-uses urban soils. *Int. J. Environ. Anal. Chem.* <https://doi.org/10.1080/03067319.2021.1977286>.
- Jahan, C.S., Islam, M.A., Mazumder, Q.H., Asaduzzaman, M., Islam, M.M., Islam, M.O., Sultana, A., 2005. Evaluation of depositional environment and aquifer condition in the Barind area, Bangladesh, using gamma ray well log data. *J. Geol. Soc. India* 70, 1070–1076.
- Jin, Z., Ding, S., Sun, Q., Gao, S., Fu, Z., Gong, M., Lin, J., Wang, D., Wang, Y., 2019. High resolution spatiotemporal sampling as a tool for comprehensive assessment of zinc mobility and pollution in sediments of a eutrophic lake. *J. Hazard. Mater.* 364, 182–191.
- Journel, A.G., Huijbregts, C.J., 1978. *Mining Geostatistics*. Academic Press, London.
- Kabir, M.H., Islam, M.S., Hoq, M.E., Tusher, T.R., Islam, M.S., 2020. Appraisal of heavy metal contamination in sediments of the Shitalakhya River in Bangladesh using pollution indices, geo-spatial, and multivariate statistical analysis. *Arab. J. Geosci.* 13 (21), 1135. <https://doi.org/10.1007/s12517-020-06072-5>.
- Kamrani, S., Rezaei, M., Amiri, V., Saberinasar, A., 2016. Investigating the efficiency of information entropy and fuzzy theories to classification of groundwater samples for drinking water purposes: Lenjanat Plain, Central Iran. *Environ. Earth Sci.* 75, 1370. <https://doi.org/10.1007/s12665-016-6185-1>.
- Karunanidhi, D., Aravinthasamy, P., Subramani, T., Setia, R., 2022. Effects of COVID-19 pandemic lockdown on microbial and metals contaminations in a part of Thirumanimuthar

- River, South India: a comparative health hazard perspective. *J. Hazard. Mater.* 416, 125909. <https://doi.org/10.1016/j.jhazmat.2021.125909>.
- Kazakisa, N., Matiatos, I., Ntonaa, M.M., et al., 2020. Origin, implications and management strategies for nitrate pollution in surface and ground waters of Anthemountas basin based on a  $\delta^{15}\text{N-NO}_3^-$  and  $\delta^{18}\text{O-NO}_3^-$  isotope approach. *Sci. Total Environ.* 724, 138112.
- Kelly, W.P., 1940. Permissible composition and concentration of irrigated waters. *Proc. ASCF* 66, 607.
- Khan, R., Islam, H.M.T., Islam, A.R.M.T., 2021. Mechanism of elevated radioactivity in Teesta River basin from Bangladesh: radiochemical characterization, provenance and associated hazards. *Chemosphere* 264, 128459. <https://doi.org/10.1016/j.chemosphere.2020.128459>.
- Khan, R., Saxena, A., Shukla, S., Selvam, S., Goel, P., 2021. Effect of COVID-19 lockdown on the water quality index of River Gomti, India, with potential hazard of faecal-oral transmission. *Environ. Sci. Pollut. Res.* <https://doi.org/10.1007/s11356-021-13096->
- Khan, R., Islam, H.M.T., Apon, M.A.S., Islam, A.R.M.T., et al., 2022. Environmental geochemistry of higher radioactivity in a transboundary Himalayan river sediment (Brahmaputra, Bangladesh): potential radiation exposure and health risks. *Environ. Sci. Pollut. Res.* <https://doi.org/10.1007/s11356-022-19735-5>.
- Kim, Y., Kong, I., Park, H., Kim, H.J., Kim, L.J., Um, M.J., Green, P.A., Vörösmarty, C.J., 2018. Assessment of regional threats to human water security adopting the global framework: a case study in South Korea. *Sci. Total Environ.* 637–638, 1413–1422.
- Kubra, K., Mondol, A.H., Ali, M.M., Palash, M.A.U., Islam, M.S., Islam, A.R.M.T., Bhuyani, M.S., Ahmed, A.S.S., Rahman, M.Z., Rahman, M.M., 2022. Pollution level of trace metals (As, Pb, Cr and Cd) in the sediment of Rupsha River, Bangladesh: assessment of ecological and human health risks. *Front. Environ. Sci.* <https://doi.org/10.3389/fenvs.2022.778544>.
- Kumar, S., Islam, A.R.M.T., Islam, H.M.T., Hasanuzzaman, M., Ongoma, V., Khan, R., Mallick, J., 2021. Water resources pollution associated with risks of heavy metals from Vatukoula Goldmine region, Fiji. *J. Environ. Manag.* 293, 112868. <https://doi.org/10.1016/j.jenvman.2021.112868>.
- Kumar, S., Islam, A.R.M.T., Hasanuzzaman, M., Salam, R., Islam, M.S., Khan, R., Rahman, M.S., Pal, S.C., Ali, M.M., Idris, A.M., Gustave, W., Elbeltagi, A., 2022. Potentially toxic elemental contamination in Wainivesi River, Fiji impacted by gold-mining activities using chemometric tools and SOM analysis. *Environ. Sci. Pollut. Res.* <https://doi.org/10.21203/rs.3.rs-941620/v1>.
- Li, Y., Chen, H., Song, L., Wu, J., Sun, W., Teng, Y., 2021. Effects on microbiomes and resistomes and the source-specific ecological risks of heavy metals in the sediments of an urban river. *J. Hazard. Mater.* 409, 124472.
- Liu, Q., Jia, Z., Li, S., Hu, J., 2019. Assessment of heavy metal pollution, distribution and quantitative source apportionment in surface sediments. *Chemosphere* 225, 829–838.
- Mahipal, S.S., Rajeev, K., Prashant, A., 2018. Arsenic in water contamination & toxic effect on human health: current scenario of India. *J. Forensic Sci. Crim. Investig.* 10 (2), 555781. <https://doi.org/10.19080/JFSCI.2018.10.555781>.
- Mohan, S.V., Nithila, P., Reddy, S.J., 1996. Estimation of heavy metal in drinking water and development of heavy metal pollution index. *J. Environ. Sci. Health A31*, 283–289.
- Mukherjee, P., Pramanick, P., Zaman, S., Mitra, A., 2020. Eco-restoration of River Ganga water quality during COVID-19 lockdown period using Total Coliform (TC) as a proxy. *J. Cent. Regul. Stud., Gov. Public Policy* 75–82.
- Nasher, N.N.R.N., Islam, M.Y., 2021. COVID-19 Lockdown Effects on Water Turbidity of a Highly Polluted Lake in Dhaka City, Bangladesh. *67(2)*, pp. 122–133. <https://doi.org/10.48008/ngji.1765> Book 2254.
- Nguyen, B.T., Do, D.D., Nguyen, T.X., Nguyen, V.N., Nguyen, D.T.P., Nguyen, M.H., Truong, H.T.T., Dong, H.P., Le, A.H., Bach, Q.-V., 2020. Seasonal, spatial variation, and pollution sources of heavy metals in the sediment of the Saigon River, Vietnam. *Environ. Pollut.* 256, 113412.
- Otmami, A., Benchrif, A., Tahri, M., Bounakhla, M., Chakir, E.M., El Bouch, M., Krombi, M., 2020. Impact of covid-19 lockdown on PM10 and NO2 concentrations in sale city (Morocco). *Sci. Total Environ.* 735, 139541.
- Paliwal, K.V., 1972. Irrigation With Saline Water. Monogram no. 2, New Series. 198. IARI, New Delhi.
- Pant, R.R., Bishwakarma, K., et al., 2021. Imprints of COVID-19 lockdown on the surface water quality of Bagmati river basin Nepal. *J. Environ. Manag.* 289. <https://doi.org/10.1016/j.jenvman.2021.112522>.
- Patel, P.P., Mondal, S., Ghosh, K.G., 2020. Some respite for India's dirtiest river? Examining the Yamuna's water quality at Delhi during the COVID-19 lockdown period. *Sci. Total Environ.* 744, 140851.
- Pawlowsky-Glahn, V., Egozcue, J.J., Tolosana-Delgado, R., 2015. Modeling and Analysis of Compositional Data. John Wiley & Sons Ltd, The Atrium, Southern Gate, Chichester, West Sussex, PO19 8SQ, United Kingdom, p. 272 9781118443064.
- Proshad, R., Kormoker, T., Abdullah Al, M., Islam, M.S., Khadka, S., Idris, A.M., 2022. Receptor model-based source apportionment and ecological risk of metals in sediments of an urban river in Bangladesh. *J. Hazard. Mater.* 423, 127030. <https://doi.org/10.1016/j.jhazmat.2021.127030>.
- Qu, L., Huang, H., Xia, F., Liu, Y., Dahlgren, R.A., Zhang, M., Mei, K., 2018. Risk analysis of heavy metal concentration in surface waters across the rural-urban interface of the Wen-Rui Tang River, China. *Environ. Pollut.* 237, 639–649.
- Ravenscroft, P., Burgess, W.G., Ahmed, K.M., Burren, M., Perrin, J., 2005. Arsenic in groundwater of the Bengal Basin, Bangladesh: distribution, field relations, and hydrogeological setting. *Hydrogeol. J.* 13, 727–751. <https://doi.org/10.1007/s10040-003-0314-0>.
- Reimann, C., Filzmoser, P., Fabian, K., Hron, K., Birke, M., Demetriades, A., Dinelli, E., Ladenberger, A., 2012. The concept of compositional data analysis in practice — total major element concentrations in agricultural and grazing land soils of Europe. *Sci. Total Environ.* 426, 196–210. <https://doi.org/10.1016/j.scitotenv.2012.02.032>.
- Reimann, K.U., 1993. Geology of Bangladesh. Schweizerbart, Stuttgart, Germany.
- Rendana, M., Idris, W.M.R., Rahim, S.A., 2022. Effect of COVID-19 Movement Control Order Policy on Water Quality Changes in Sungai Langat, Selangor, Malaysia within Distinct Land Use Areas. *Sains Malaysiana* 51 (5), 1587–1598. <https://doi.org/10.17576/jsm-2022-5105-26>.
- Richards, L.A., 1954. Diagnosis and Improvement of Saline Alkali Soils. 60. US Department of Agriculture, p. 160 Hand Book.
- Sarkar, B., Islam, A., 2020. Drivers of water pollution and evaluating its ecological stress with special reference to macrovertebrates (fish community structure): a case of Churni River, India. *Environ. Monit. Assess.* 192 (1), 1–31. <https://doi.org/10.1007/s10661-019-7988-9>.
- Sarkar, B., Islam, A., Majumder, A., 2021. Seawater intrusion into groundwater and its impact on irrigation and agriculture: Evidence from the coastal region of West Bengal, India. *Reg. Stud. Mar. Sci.* 44, 101751. <https://doi.org/10.1016/j.risma.2021.101751>.
- Sarkar, S., Roy, A., Bhattacharjee, S., Shit, P.K., Bera, B., 2021. Effects of COVID-19 lockdown and unlock on health of Bhutan-India-Bangladesh trans boundary rivers. *J. Hazard. Mater. Adv.* 4 (2021), 100030. <https://doi.org/10.1016/j.hazadv.2021.100030>.
- Selvam, S., Jesuraja, K., Venkatraman, S., Chung, S.Y., Roy, P.D., Muthukumar, P., Kumar, M., 2020. Imprints of pandemic lockdown on subsurface water quality in the coastal industrial city of Tuticorin, south India: a revival perspective. *Sci. Total Environ.* 139848. <https://doi.org/10.1016/j.scitotenv.2020.139848>.
- Shah, D.N., Devi, R., Shah, T., Rijal, D., Sharma, S., 2020. Impacts of COVID-19 and Nationwide Lockdown on River Ecosystems in Nepal, pp. 56–58 <https://doi.org/10.34297/AJBSR.2020.10.001474> Accessed date: 08 January 2021.
- Shammi, M., Bodrud-Doza, M., Islam, A.R.M.T., Rahman, M.M., 2020. COVID-19 pandemic, socio-economic crisis and human stress in resource-limited settings: a case from Bangladesh. *Heliyon* 6 (5), e04063. <https://doi.org/10.1016/j.heliyon.2020.e04063> Elsevier, Scopus Index.
- Shammi, R.S., Hossain, M.S., Kabir, M.H., Islam, M.S., Taj, M.T.I., Islam, M.S., Sarker, M.E., Hossain, M.S., Idris, A.M., 2022. Hydrochemical appraisal of surface water from a subtropical urban river in southwestern Bangladesh using indices, GIS, and multivariate statistical analysis. *Environ. Sci. Pollut. Res.* <https://doi.org/10.1007/s11356-022-22384-3>.
- Sharma, S., Zhang, M., Anshika Gao, J., Zhang, H., Kota, S.H., 2020. Effect of restricted emissions during COVID-19 on air quality in India. *Sci. Total Environ.* 728, 138678.
- Shi, J., Wang, H., Xu, J., Wu, J., Liu, X., Zhu, H., Yu, C., 2007. Spatial distribution of heavy metals in soils: a case study of Changxing, China. *Environ. Geol.* 52 (1), 1–10. <https://doi.org/10.1007/s00254-006-0443-6>.
- Shil, S., Singh, U.K., Mehta, P., 2019. Water quality assessment of a tropical river using water quality index (WQI), multivariate statistical techniques and GIS. *Appl. Water Sci.* 9 (7), 168. <https://doi.org/10.1007/s13201-019-1045-2>.
- Shukla, T., Sen, I.S., Boral, S., Sharma, S., 2021. A Time-Series Record During COVID-19 Lockdown Shows the High Resilience of Dissolved Heavy Metals in the Ganga River. ACS Publications Collection <https://doi.org/10.1021/acs.estlett.0c00982>.
- Siddique, A.B.M., Islam, A.R.M.T., et al., 2022. Multivariate statistics and entropy theory for irrigation water quality and entropy-weighted index development in a subtropical urban river, Bangladesh. *Environ. Sci. Pollut. Res.* 29, 8577–8596. <https://doi.org/10.1007/s11356-021-16343-7>.
- Singh, A.K., Mondal, G.C., Kumar, S., Singh, T.B., Sinha, A., 2008. Major ion chemistry, weathering processes and water quality assessment in upper catchment of Damodar River basin, India. *Environ. Geol.* 54, 745–758.
- Sojobi, A.O., 2016. Evaluation of groundwater quality in a rural community in North Central of Nigeria. *Environ. Monit. Assess.* 188, 192–205.
- Sun, C., Zhang, Z., Cao, H., Xu, M., Xu, L., 2019. Concentrations, speciation, and ecological risk of heavy metals in the sediment of the Songhua River in an urban area with petrochemical industries. *Chemosphere* 219, 538–545.
- Sundaray, S.K., Nayak, B.B., Bhatta, D., 2009. Environmental studies on river water quality with reference to suitability for agricultural purposes: Mahanadi River estuarine system, India — a case study. *Environ. Monitor. Assess.* 155, 227–243. <https://doi.org/10.1007/s10661-008-0431-2>.
- Thornton, I., Farago, M.E., 2012. The geochemistry of arsenic. In: Abernathy, C.O., Calderon, R.L., Chappell, W.R. (Eds.), *Arsenic Exposure and Health Effects*. Chapman & Hull, London, pp. 1–16.
- Tokatli, C., Varol, M., 2021. Impact of the COVID-19 lockdown period on surface water quality in the Meriç-Ergene River Basin, Northwest Turkey. *Environ. Res.* 197, 111051.
- Tokatli, C., Titiz, A.M., Uğurluoğlu, A., Islam, A.R.M.T., et al., 2022. Assessment of the effects of COVID-19 lockdown period on groundwater quality of a significant rice land in an urban area of Türkiye. *Environ. Sci. Pollut. Res.* <https://doi.org/10.1007/s11356-022-20959-8>.
- Uddin, R., Huda, N.H., 2011. Arsenic poisoning in Bangladesh. *Oman Med. J.* 26 (3), 207. <https://doi.org/10.5001/omj.2011.51>.
- UNICEF, 2009. Bangladesh National Drinking Water Quality Survey. Bangladesh Bureau of Statistics, Planning Division, Ministry of Planning, Government of the People's Republic of Bangladesh. <https://washdata.org/sites/default/files/documents/reports/Bangladesh-2009-MICS-water-quality-report>.
- USEPA, 2021. National Primary Drinking Water Regulations. Accessed date: 08 January 2021 <https://www.epa.gov/groundwater-and-drinking-water/national-primary-drinking-water-regulations#Inorganic>.
- USEPA (US Environmental Protection Agency), 2009. National Primary/secondary and Drinking Water Regulations Washington, D.C.
- Ustaoglu, F., Islam, M.S., 2020. Potential toxic elements in sediment of some rivers at Giresun, Northeast Turkey: a preliminary assessment for ecotoxicological status and health risk. *Ecol. Indic.* 113, 106237.
- Ustaoglu, F., Tepe, Y., 2019. Water quality and sediment contamination assessment of Pazarsuyu Stream, Turkey using multivariate statistical methods and pollution indicators. *Int. Soil Water Conserv. Res.* 7, 47–56.
- Varol, M., 2019. Arsenic and trace metals in a large reservoir: seasonal and spatial variations, source identification and risk assessment for both residential and recreational users. *Chemosphere* 228, 1e8.
- WHO, 2011. Guidelines for Drinking Water Quality. fourth ed. World Health Organization, Geneva.

- Wu, B., Zhao, D.Y., Jia, H.Y., Zhang, Y., Zhang, X.X., Cheng, S.P., 2009. Preliminary risk assessment of trace metal pollution in surface water from Yangtze River in Nanjing Section, China. *Bull. Environ. Contam. Toxicol.* 82, 405–409.
- Xiao, J., Wang, L., Deng, L., Jin, Z., 2019. Characteristics, sources, water quality and health risk assessment of trace elements in river water and well water in the Chinese Loess Plateau. *Sci. Total Environ.* 650, 2004–2012.
- Xiong, B., Li, R., Johnson, D., Luo, Y., Xi, Y., Ren, D., Huang, Y., 2021. Spatial distribution, risk assessment, and source identification of heavy metals in water from the Xiangxi River, Three Gorges Reservoir Region. *China Environ. Geochem. Health* 43 (2), 915–930.
- Yan, N., Liu, W., Xie, H., Gao, L., Han, Y., Wang, M., Li, H., 2016. Distribution and assessment of heavy metals in the surface sediment of Yellow River, China. *J. Environ. Sci.* 39, 45–51.
- Yeazdani, S.M.G., 2016. State of drinking water and its management aspects in Dhaka city. *J. Nepal Geol. Soc.* 50, 59–64.
- Yunus, A.P., Masago, Y., Hijioka, Y., 2020. COVID-19 and surface water quality: improved lake water quality during the lockdown. *Sci. Total Environ.* 731, 139012.
- Zakir, H.M., Hasan, M.N., Quadir, Q.F., Sharmin, S., Ahmed, I., 2013. Cadmium and lead pollution in sediments of midstream of the river Karatoa in Bangladesh. *Int. J. Eng. Sci.* 2, 34–42.
- Zhao, Q., Bai, J., Gao, Y., Zhang, G., Lu, Q., Jia, J., 2022. Heavy metal contamination in soils from freshwater wetlands to salt marshes in the Yellow River Estuary, China. *Sci. Total Environ.* 774, 145072.